WRINKLING OF WEBS APPROACHING HEATED ROLLERS

By

SAIKIRAN DIVAKARUNI

Bachelor of Engineering in Mechanical Engineering
Anna University
Chennai, Tamil Nadu, India
2006

Submitted to the Faculty of the
Graduate College of the
Oklahoma State University
in partial fulfillment of
the requirements for
the Degree of
MASTER OF SCIENCE
May, 2011

WRINKLING OF WEBS APPROACHING HEATED ROLLERS

Dissertation Approved:

Dr.J.K.Good

Thesis Adviser

Dr.Raman P.Singh

Dr.Kaan Kalkan

Dr. Mark E. Payton

Dean of the Graduate College

ACKNOWLEDGMENTS

I would like to express my sincere gratitude and thanks to my advisor Dr.J.K.Good for his continuous support and assistance in my thesis work. He guided me with persistent encouragement and profound technical knowledge which enhanced my spirit to do research in the specified topic. This work would not have been possible without his guidance and support.

I would like to thank my committee members Dr.R.P Singh and Dr.Kalkan for their advice and support in my work. I am fortunate to have them as my committee members.

I would like to thank Mr.Ron Markum for his support during my research work and his help in conducting the experiments. I would like to thank my family for their immense and continuous support in my life.

Also I would like to thank all my group members for their help and support offered during my research work.

TABLE OF CONTENTS

Chapter Page

Chapter Page

LIST OF TABLES

Table Page

LIST OF FIGURES

CHAPTER I

INTRODUCTION

Understanding Web and Web Handling

Web is a material whose thickness is small compared to its width and length. Papers, plastic films, woven materials, and metal foils that are in continuous form are examples of web materials. Generally, these web materials are stored as wound rolls. Wound webs are unwound and made to pass over several rollers before they are processed into different end products. The act of transporting webs through processes is commonly referred as web handling. Some examples of web processes include: printing, drying, slitting, coating, embossing, calendaring, and laminating. These processes are performed to add a value to web prior to its conversion into a final/end product.

There are several issues that arise while handling webs during these processes. Webs are generally unwound with a certain tension, and that tension is applied to webs in machine direction (MD). Machine direction is the direction in which web travels. Cross machine direction (CMD) is the direction that is perpendicular to the machine direction. Instabilities in webs are caused due to compressive stresses that are induced during transportation. Web instabilities can be classified into troughs and wrinkles.

Web Handling Terminologies

Troughs are small out-of-plane deformations that form over web span between two rollers. These small web deformations do not generally affect the quality of the end product. However, if these troughs exceed certain amplitude, they can induce web wrinkles when they are passed over rollers. This wrinkling often affects the quality of web and web processes. Thus, trough is a web instability that arises on free span and wrinkle is that of on roller.

These troughs and wrinkles are induced due to several reasons [4, 7, 10, and 11]; some of the reasons that were found through studies earlier are:

1. Roller misalignment
2. Diameter variation of a roller
3. Tapered roller
4. Web lateral motion
5. Decrease in web tension
6. Difference in web thickness
7. Discontinuities in the web material

Some web processing machines often incorporate heat as a means of drying for coating and other processes. Since webs are very thin, they have very low thermal mass. As a result, they get heated up quickly causing an expansion in MD and CMD directions.

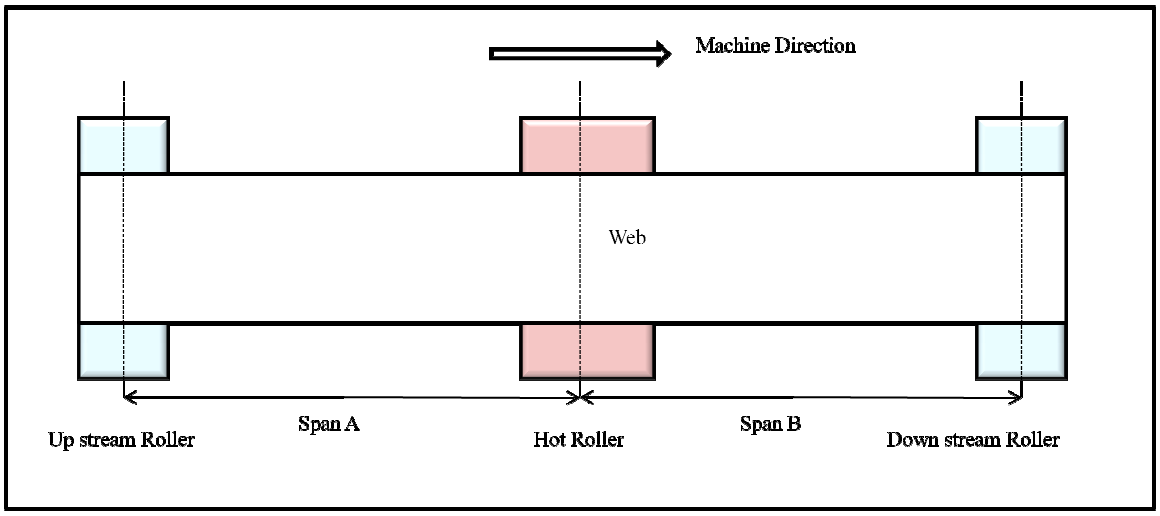

Fig 1.1 – A two span web system with a hot roller.

Scope of the Research

In this research, study is done on the interaction between webs and rollers; with rollers having temperatures higher than webs. The investigation includes both, tests and modeling aspects. The scope of this research is to define conditions where the interaction between heated roller and web will produce web instability in the form of troughs and wrinkles.

CHAPTER II

Review of Literature

Theory governing the lateral dynamics of web traveling through a web line was first studied by Shelton [1]. He discussed steering of web due to a misaligned roller. He developed fundamentals of web behavior including a slack edge criterion and a zero internal web moment boundary condition for a web approaching downstream roller. The principle of normal entry of a web approaching a downstream roller was stated by Shelton.

The structural behavior of web wrinkle passing over a cylinder roller using finite element technique was investigated by Friedrich and Good [2]. They assumed the material to be homogenous and isotropic, and determined the relative effects of various geometric and material parameters on the wrinkling stability. Each and every parameter was varied in different iterations keeping others constant to study its effect on the wrinkling stability. Issues such as web tearing and longitudinal web creasing were considered with corrective guidelines in this study.

The failure criteria for predicting the onset of shear troughs in a free span of a web was established by Gehlbach et al [3]. Here the web was not allowed to slip at the roller that is in immediate upstream of the misaligned roller. The shear stresses due to misalignment, coupled with a web line tension, resulted in a compressive 2nd principal stress that was responsible for buckling of the web. This compressive stress was then

compared against Timoshenko's plate buckling theory criteria [5]. When a misalignment was sufficient to produce a compressive principal stress with a higher negative value than Timoshenko's buckling criteria, web buckled or troughs were assumed to be present. Experiments were performed with different web thickness, web line velocities, and length to width aspect ratios (a/b). Good agreement between modeling and test was found.

Biesel and Good [4] extended the previous work of Gehlbach to buckling of orthotropic webs due to a misaligned roller. A critical buckling equation for predicting troughs was derived,

$$\sigma_{ycr} = -2\left(\sigma_{e+}\sqrt{\sigma_e^2 + \sigma_e\sigma_x}\right) \qquad \{2.1\}$$

where: σ_{ycr}= CMD stress required to induce web troughs.

σ_x = MD Stress due to web tension.

and $\sigma_e = \frac{\pi^2 D}{a^2 h}$ where, $D = \frac{Et^3}{12(1-\vartheta^2)}$ $\{2.2\}$

and a is the span length , h is the web thickness and E and υ are Young's modulus and Poisson's ratio of the web respectively.

The critical buckling stress to induce wrinkles in cylindrical shells was predicted by Timoshenko [5],

$$\sigma_{ycr} = \frac{-h\,E}{R\sqrt{3(1-\vartheta^2)}} \qquad \{2.3\}$$

Where, R is the radius of the cylindrical shell.

Buckling of webs in free span and rollers due to lateral compressive forces was studied by Shelton [6]. A buckling criterion was developed for the web on the roller. The roller was assumed as a pressurized cylindrical shell. He analyzed the wrinkling behavior of web due to change in tension along the roller, temperature, and moisture levels. Viscoelastic memory of plastic webs, bending of wound rolls, and roller deflections were also considered as possible sources for compressive stresses. However, no tests or simulation were done related to temperature variation across the web passing over hot rollers.

A finite element code to simulate wrinkling patterns in the web due to non-uniform transport conditions was developed by Bensen et al [7]. Wrinkling of very thin webs under different edge displacement conditions was examined. The code was based on tension field theory. A finite element code with wrinkling analysis (FEWA) was developed which utilized the wrinkling strain method. This assumes that the out-of- plane deflection had relieved compressive stress across wrinkle and there was strain associated with this deflection. The algorithm can be modified depending upon whether individual elements exhibit taut or wrinkled behavior. However, this code was unable to predict onset of troughs or wrinkling.

A closed form solution for predicting wrinkles due to web twist were developed by Good and Straughan [8]. The Rayleigh-Ritz method was employed to develop the stress profiles throughout the membrane under twist using Airy stress functions. The CMD stress due to twist from the analysis was equated to the critical value required to buckle the cylindrical shell of web upon the roller surface to predict the onset of wrinkles. This theory was experimentally verified for two thicknesses of PET with varied span lengths.

A finite element method to predict web wrinkles due to misalignment of a downstream roller in a web span was used by Webb [9]. He had used wrinkling membrane elements to model the free span. This model was also verified experimentally. This method was later improved by Beisel [10] who applied it to spans with downstream misaligned rollers and tapered rollers. Beisel used finite element models to predict troughs and wrinkles in uniform webs. He was successful in this for the cases of webs approaching tapered and misaligned rollers. Beisel employed a commercial Finite Element Code (COSMOS) in his research. Analytical expressions for the critical taper and critical misalignment required for trough formation were derived. In these models, he used the boundary conditions established by Shelton [1]. He also considered the normal entry rule. By applying shear forces in CMD, the taper and misaligned rollers were simulated. The applied forces were increased in small increments in non linear analysis because wrinkling membrane elements were employed. Shear force was increased until the critical buckling stress was reached. The Timoshenko shell buckling criteria was applied to model web wrinkling on roller. For both models, the experimental results

matched well with the simulation results. This study was the first in the literature in presenting a method by which both troughs and wrinkles in webs could be predicted.

The effects of voids such as circular or elliptical holes on stability of webs were investigated by Mallya [11]. Voids in webs occur during formation process, or sometimes they are intentionally cut to satisfy the needs of a final web product. When these voids approach the downstream roller, troughs form, and in turn induce wrinkles. The CMD compressive stresses in the web over the roller became more compressive, as the void and the associated troughs were near the roller. This case was modeled in COSMOS using the finite element technique outlined by Beisel [10]. The model results were verified with experimental tests.

A finite element model to predict wrinkles in webs due to non-uniform length across the width was developed by Kara [12]. The finite element modeling method used by Beisel [10] was modified to predict occurrence of wrinkle due to length non-uniformity. The model was verified experimentally, and the length variation across the web width was simulated using thermo-elastic response of the web to a particular temperature distribution.

Research Objective

The objective of this research is to define the conditions where the interaction between the webs and rollers at higher temperatures than that of webs will produce web instability in the form of troughs or wrinkles. Based on the literature survey this work is novel because, no work has been done with regard to web interaction with heated rollers. In this research a heated roller is installed in the web line to study the effects of temperature on web instability.

CHAPTER III

EXPERIMENTAL SETUP & RESULTS

Small Scale Winder

A small scale winder setup was used to perform tests to view troughs and wrinkles on web passing over heated roller. A digital tension readout-and-controller, manufactured by Magnetic Power System Inc, was used to control tension in web line. Digital microprocessor based control system was adopted in the readout instrument. A required tension value can be inputted using the input panel on the tension control. The unwind was attached with a hysteresis brake, manufactured by Magtrol, Inc (Model – HB-5500-1), that was used to apply tension during unwinding. A cantilever web tension sensor (Tension measurement), manufactured by Magnetic Powers System (Model CL250), was installed along with one of the rollers in the web line. Cantilever tension sensors were designed to support cantilever idler rollers that had one side frame and were able to accurately measure and control tension in a narrow moving web. They provide feedback signal to the digital tension readout-and-controller that controls the brake on the unwind roller maintaining the required tension. A constant tension of 4 lbs was maintained throughout the tests.

FIFE electromechanical web guide was installed in the web line to guide the web to a constant lateral position. This electro-mechanical web guide was used to steer the web on the next roller. The position of the exiting web was set by adjusting the sensor position. This sensor monitors the web position, and if the web leaves the

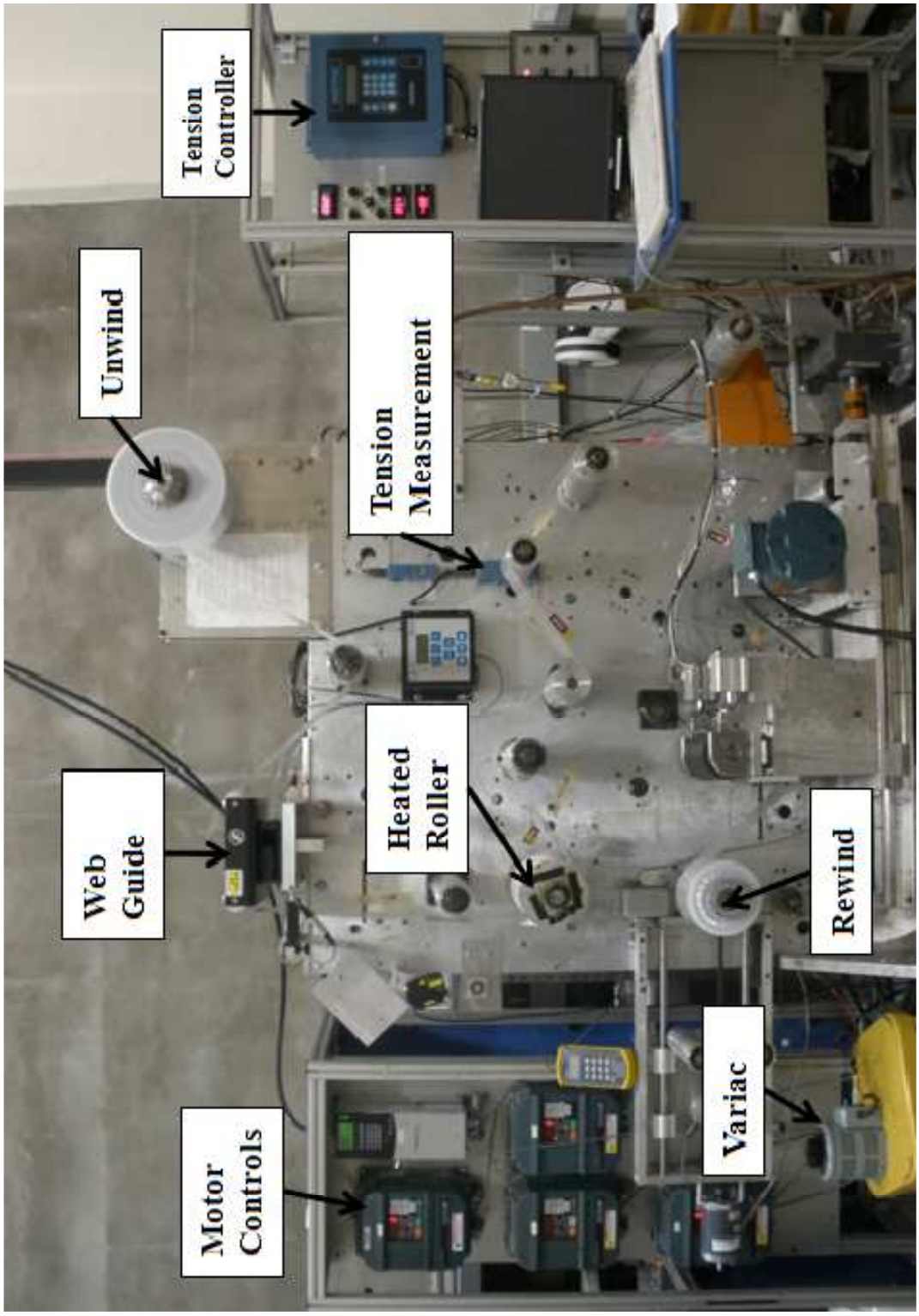

Fig 3.1: - Small scale winder setup.

required position, an error signal is generated which gives feed back to the FIFE guide to align it to required position so that the web is guided properly onto next roller.

The angular velocity of the rewind roller was controlled by an A.C Driven speed controller (Motor control), manufactured by Reliance Electric (Model: GV 3000). The experiments were run by setting the speed at 50 RPM on the speed control. The web line velocity was calculated using RPM value set in the speed control panel and rewind roller diameter. Since the rewind roller diameter was 3 inches, the web velocity was calculated to be 70.68 feet/min.

The Heated Roller

A heated roller was designed and built by Mr. Ron Markum. He also helped to install this roller in the web line. Its position on the machine is after the web guide, so that the web will be guided properly over the heated roller. This roller is a hollow aluminum cylinder with an outer diameter of 5.6". The roller was mounted on a shaft to which a heating element was fixed. Oil was poured into the cylinder to ¾th of its volume through an inlet port which is closed by an Allen screw. The oil used for this experiment was carefully chosen as it has flash point above 400^{o}F. The maximum temperature targeted in this experiment was 140^{o}F to 150^{o}F. Figures 3.2 and 3.3 show a photo and cross-sectional image of the heated roller.

Fig 3.2: - Heated Roller

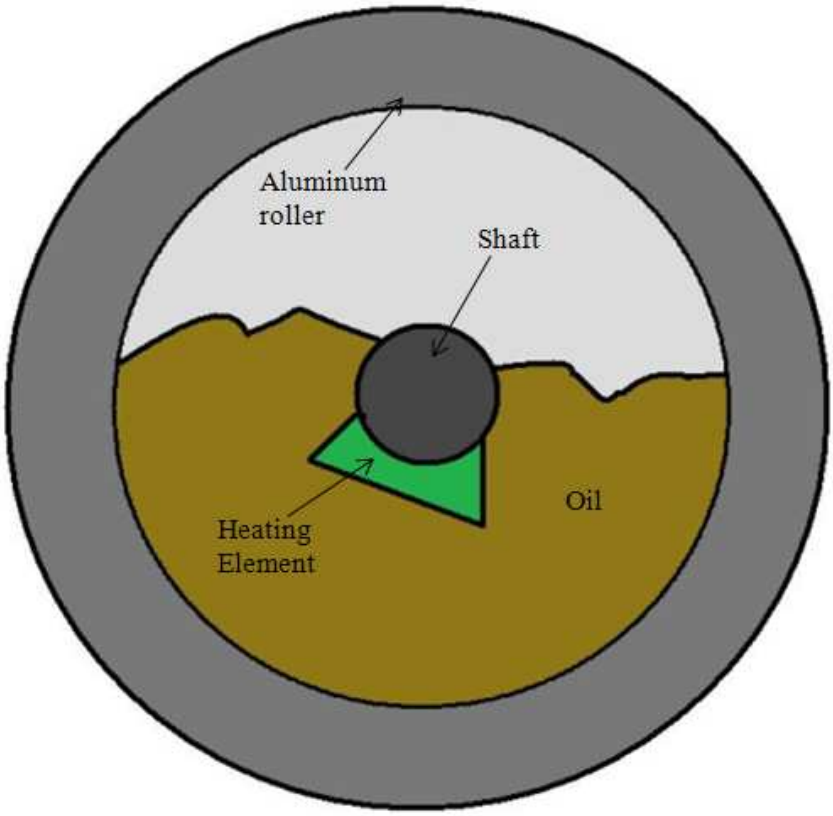

Fig 3.3: - Heated Roller cross-sectional view.

The electric heating element was powered by a Variac to attain the desired temperature. Once the heating element started heating the oil bath, heat was transferred to the roller shell through conduction.

Static Test

Low Density Polyethylene (LDPE) web was cut to a length of 18 inches. Metal strips with hole in the center were taped at both the ends of the web. Two hinges were mounted on the holes of the ends to carry the dead weights (4 lb). The LDPE web was then draped over the bare aluminum roller surface as shown in Fig 3.4. The heated roller was restrained for its rotation.

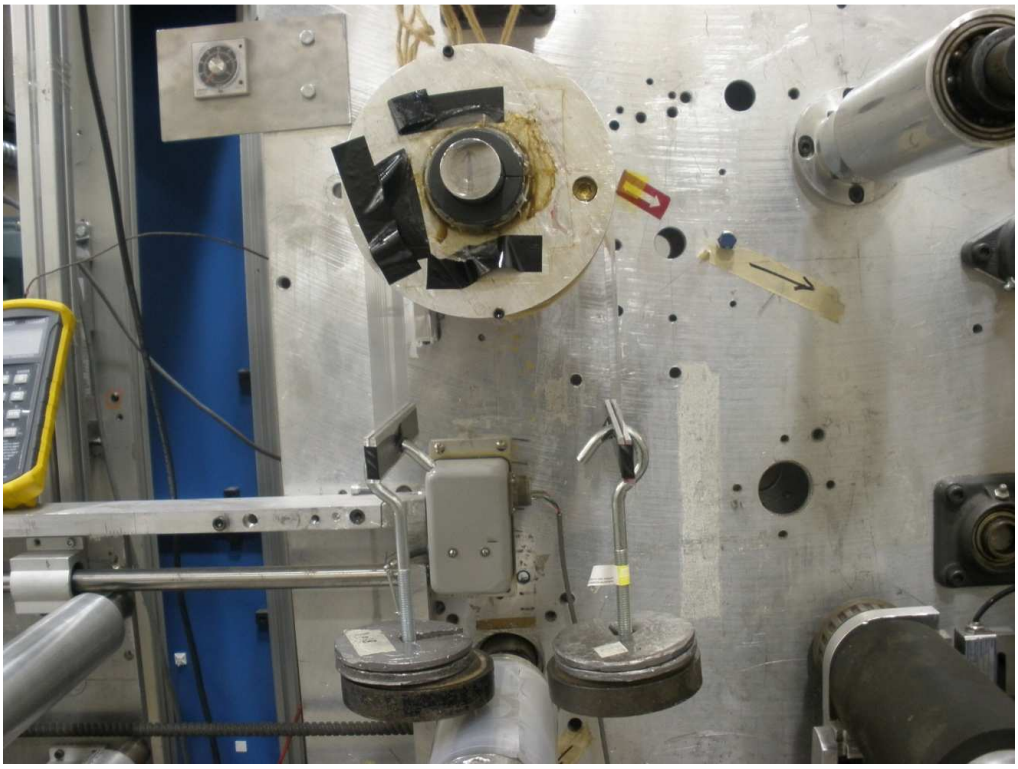

Fig 3.4: LDPE web draped over bare aluminum roller with dead weights.

A dead weight of 4 lbs was hung on each side of the web to simulate web tension. The temperature on the draped web surface was checked at three locations (Fig 3.5) using a thermocouple. Later, the temperature of the roller was slowly increased to 120^{o}F and the same measurements were recorded on the roller and web surfaces. Table 3.1 shows the readings.

Roller Temperature (Deg F)	Web temperature (Deg F) Location 1	Web temperature (Deg F) Location 2	Web temperature (Deg F) Location 3
75	75.3	75.5	75.5
90	90.6	90.2	90.8
100	99	99.7	100.1
115	114.7	115.2	115.8
120	119.4	120.5	120.2

Table 3.1: Comparison between bare roller temperature and web temperature in static condition.

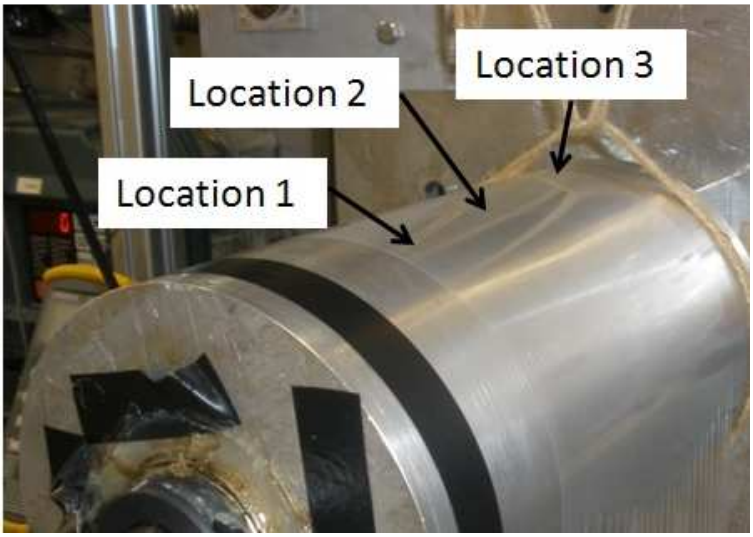

Fig 3.5: Locations where temperature was measured.

From the above readings, it is seen that the web draped over the roller surface has exactly the same temperature as the roller, and the web gets heated at the same rate as the roller is heated. This test was performed to ensure the conductivity between the roller and web was adequate for the web to achieve the temperature of the roller.

There were no buckles or wrinkles observed on the web surface during the heating process. Troughs formed at the entry and exit span of the web has been shown in Fig 3.6.

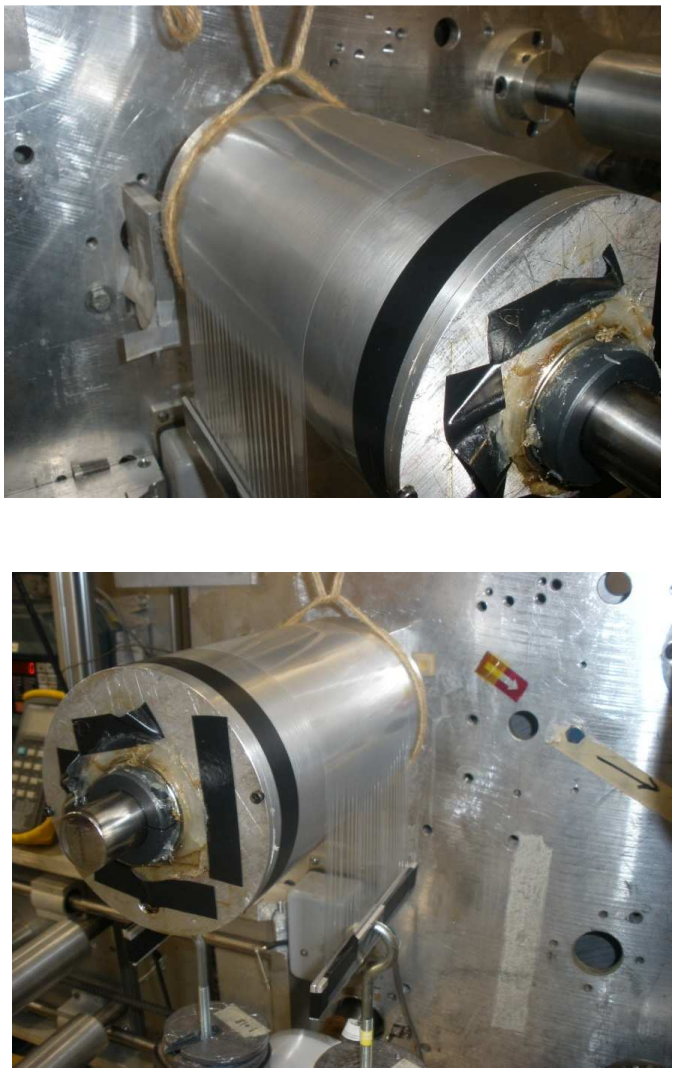

Fig 3.6: Troughs at the entry and exit, but no buckles on the roller surface.

A high friction tape (Dow 236) was stuck over the bare aluminum roller all over. The experiment was again conducted to check for proper conductivity between the roller surface with friction tape and web; with dead weights (4 lb) and sample length (18 inches). There were trough formations at the entry and exit span of the roller. No buckling or wrinkling was observed on the draped surface of the roller (Fig 3.7).

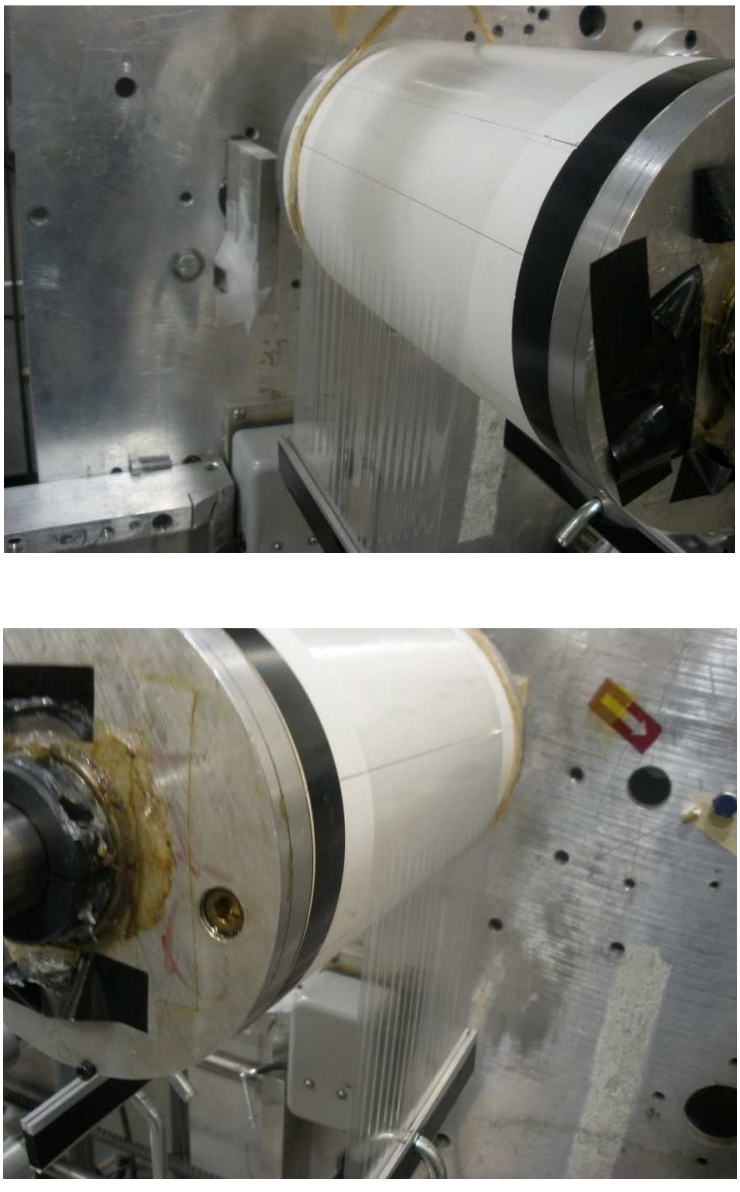

Fig 3.7: Troughs at the entry and exit, but no buckles on the roller (DOW 236) surface.

Table 3.2 shows the temperature readings,

Roller Temperature (Deg F)	Web temperature (Deg F) Location 1	Web temperature (Deg F) Location 2	Web temperature (Deg F) Location 3
73	73.4	73.6	73.1
92	91.8	92.1	92.3
100	99.9	100.2	100.2
110	110.1	110.5	110.2
120	118.3	119.4	119.1

Table3.2: Comparison between roller (Dow 236) temperature and web temperature in static condition (For locations – Ref fig 3.5)

The above readings show that the conductivity between the roller surface with friction tape and the web material was good. In both cases, bare aluminum and high friction, there will be tensile CMD stresses due to the 4 Lb web tension. The web will tend to contract in CMD as tension increased. However, frictional forces would impede this contraction and induce tension. At 75^{o}F, the web did not slip in the cross machine direction. The CMD stress can then be computed by $\sigma_y = \upsilon T$ = 200 Psi (Tension). When heated, the web did not slip and will have stresses $\sigma_y = -E\alpha\Delta T$ = -274 Psi (Compression). So the net result is that there will be a σ_y stress of -74 Psi applied.

Dynamic Test

Tests were also done under dynamic conditions (Fig 3.8) where the roller was in motion and web was moving over the heated roller. Results of dynamic web tests often differ from static tests. The normal entry boundary condition discussed by shelton[1] exists only when the web is moving. The test was first performed on the roller with high friction dow 236 tape wrapped on it. The high friction tape was then removed and the test was repeated on the bare aluminum roller. During these experiments the web temperature was measured in several locations using a thermocouple (OMEGA HH509). The temperature of the web was measured at three locations (shown in Fig 3.9) at 1" upstream to the entry of the heated roller and was found to be 80^{o}F. The temperature of the web exiting the heated roller was less than the roller temperature. When the roller was heated to 120^{o}F, the temperature of the web exiting the heated roller was measured between 110^{o}F to 115^{o}F until the web contacted the downstream roller.

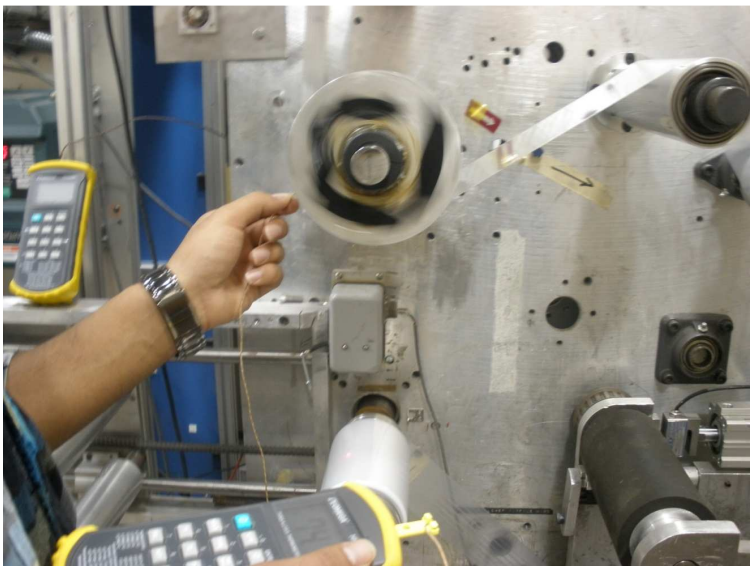

Fig 3.8: Measuring the temperature when the roller is in motion.

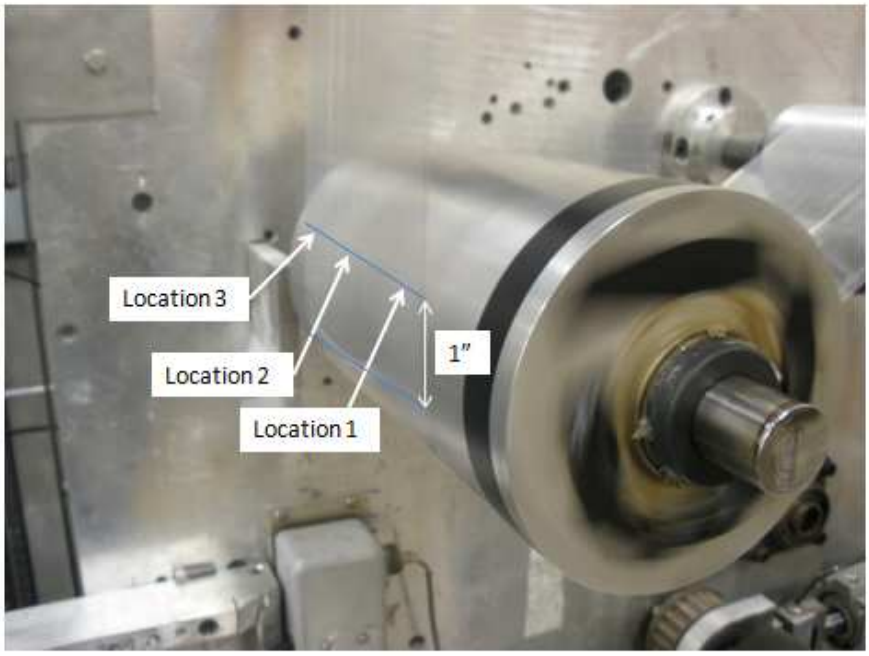

Fig 3.9: Lateral locations picture.

Tables 3.3 and 3.4 show the readings for the test where the Dow 236 tape was on the heated roller and also when the heated roller was in the bare condition.

Roller Temperature (Deg F)	Web temperature (Deg F) Location 1	Temp Just before the web touches the roller (Lateral location1)	Web temperature (Deg F) Location 2	Temp Just before the web touches the roller (Lateral location2)	Web temperature (Deg F) Location 3	Temp Just before the web touches the roller (Lateral location3)
75	76.1	76.1	76.2	76	76.4	76.2
90	91.1	77.1	92.1	78.1	91.3	77.4
100	99.7	76.4	101.4	78.6	100.9	77.8
110	108.9	80.1	108.8	80.4	109.6	80.2
120	117.9	82.7	119	81.4	118.7	82.1

Table 3.3 : Dynamic test – Temperatures of the roller (Dow 236) and web material

Roller Temperature (Deg F)	Web temperature (Deg F) Location 1	Temp Just before the web touches the roller (Lateral location1)	Web temperature (Deg F) Location 2	Temp Just before the web touches the roller (Lateral location2)	Web temperature (Deg F) Location 3	Temp Just before the web touches the roller (Lateral location3)
75	76	75.3	74.7	74.2	74.6	75.1
90	90.8	79.5	91.7	77.6	89.9	77.9
100	99.2	80.2	101.1	79.7	101	78.5
110	110.7	81	110.2	79	111	78.2
120	122.5	82.3	121.8	81	123.9	80.7

Table 3.4: Dynamic test – Temperatures of the bare aluminum roller and web material

The above reading shows that the conductivity of the roller surface with friction tape and bare aluminum roller was good with the web material.

Wrinkling Experiment

A roll of LDPE web (6” wide and 0.001” thick) was loaded on the unwind roller. The web was passed over all the rollers and finally wound on the rewind roller. The angular velocity of the rewind was set at 50 RPM and the tension was controlled at 4 lb. The speed-tension combination was arrived by conducting trial and error experiments. This was because of the fact that, the brake which is fitted onto the un-winder cogs when run at lower speeds at this particular tension. This cogging results in tension fluctuation which is undesirable. The experiment was run by increasing the temperature of the test roller (heated roller) from 75^{o}F to 120^{o}F. A noncontact infrared (IR) device (Raytek Raynger ST60 Pro Plus) was used to measure the roller temperature. The IR device

results were checked by measuring the roller temperature with a thermocouple, and when both matched, the IR device measurements were deemed correct. The experiment was started with heated roller at bare condition at 74^{o}F, and the web profile was found to be flat with no instability as shown in Fig 3.10,

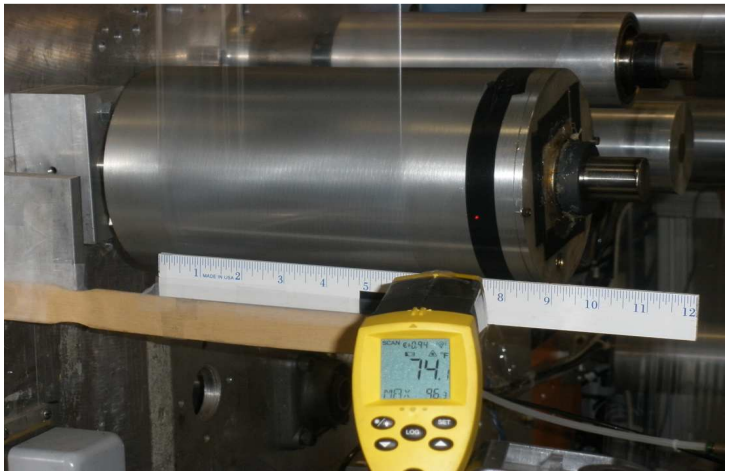

Fig 3.10: - Web profile at room temperature.

Once the roller had attained a temperature of approximately 90^{o}F, troughs started to form on the web surface near the roller as shown in fig 3.11.

Fig 3.11: - Web profile at 95^{o}F

As the temperature increased, the number of troughs and amplitude of troughs increased. When the temperature of the heated roller reached 105^{o}F, a large number of troughs and tiny wrinkles were formed at the entry of the heated roller as shown in Fig 3.12.

Fig 3.12: - Web profile at 105^{o}F

Finally, when the temperature of the heated roller had reached 120^{o}F, there were large number of troughs and wrinkles at the entry of the heated roller as shown in Fig 3.13.

Fig 3.13: - Web profile at 122^{o}F

The roller was then covered with a high friction tape (Dow 236) as shown in Fig 3.14.

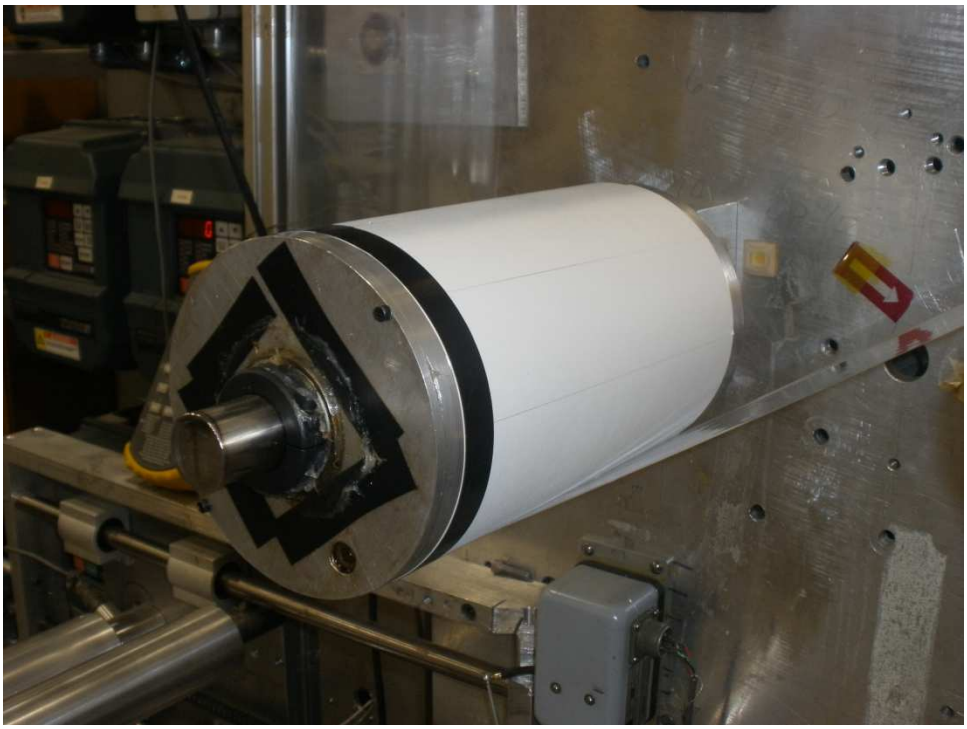

Fig 3.14: - Roller with high friction tape

The same experimental parameters were set to run the web over the high friction tape. It was found that the web was moving over the roller without any significant troughs or wrinkles at room temperature. There were only small trough formations with increase in temperature, but no wrinkles were observed as shown in Fig 3.15 and 3.16.

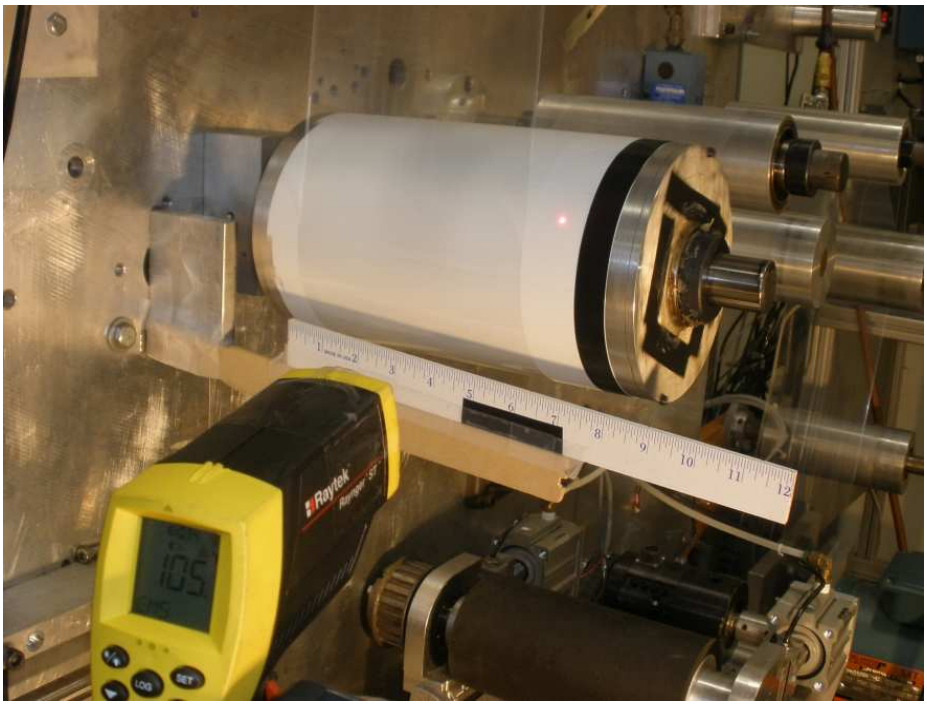

Fig3.15: - Roller with high friction tape at 105^{o}F

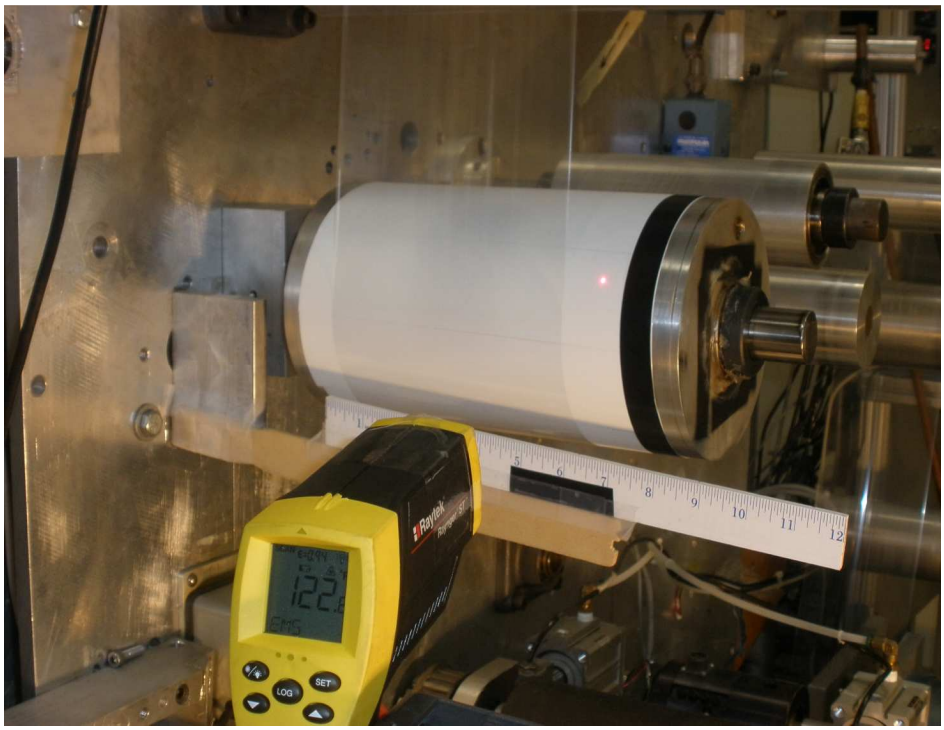

Fig 3.16: - Roller with high friction tape at 122^{o}F

Experiment to View Web Expansion

Based on the dynamic test results, a curiosity arose regarding how much the web was laterally expanding on the surface of the heated roller. Under frictionless conditions the web should expand laterally an amount $\alpha_{CMD} * \Delta T * W$. When heated roller reaches 120^{o}F. The resulting expansion should be 0.00023 in/in/ ^{o}F * (120-75) ^{o}F * 6 in, or 0.062 inch. The web was made to run over the bare aluminum roller. A steel engineering ruler with graduations of 1/64th of an inch was mounted parallel to the roller.

Initially the web readings were recorded at 75 ^{o}F. The web edge was wavy as a result of slitting and it was oscillating for 0.046 inch (3 divisions) on both the sides. These readings were captured as video for comparing similar readings taken at higher temperatures. The expansion was then captured after heating the roller to 120 ^{o}F. The test was done three times to ensure repeatability. It was observed that the web on the roller was expanding by 0.01 inch (Fig 3.17). Again theoretically the web should expand 0.062 inch due to the change in temperature. From this experiment, it was evident that, frictional forces oppose the web expansion and hence it expands only 0.01 inch when the roller surface was in bare condition.

Fig 3.17 – Web expansion test measurement on bare aluminum roller.

The experiment was then repeated with high friction tape on the cylinder surface (Fig 3.18). At 75 ^{o}F, the readings were captured at the ends of the web. After heating the roller up to 120 ^{o}F, no expansion was observed.

Fig 3.18 – Web expansion test measurement on high friction roller.

Summary of Experiments

1) From static tests, no wrinkles were observed on the either the high or low friction surface conditions when the roller temperature was increased.
2) From dynamic tests troughs appeared under low friction conditions as the temperature of the heated roller increased. As the temperature increased, the amplitude of the troughs increased. Finally at 120^{o}F wrinkles began to appear in the web on the heated roller surface. Under high friction conditions neither trough nor wrinkles were visible at similar temperature levels.
3) Temperature tests show that regardless of friction condition that the web attains the temperature of the heated roller upon contact. The web retains that temperature essentially until contact with a downstream roller (not heated) occurs.
4) Dynamic expansion testing indicated that some expansion (0.01") occurred on the bare heated roller whereas no expansion occurred in the high friction case.

Based upon these findings, it is hypothesized that the heated roller can induce troughs and wrinkles only in conditions where the web can expand laterally on the surface of the heated roller. When this occurs the web in the free span upstream of the heated roller is narrower than the web on the surface of the heated roller. This results in non-normal entry that produces troughs and finally wrinkles as the web attempts to steer inward. This hypothesis will be examined further in Chapter 4 on modeling.

Tests in Support of Modeling

To support the modeling effort, several properties needed to be measured. The first of these tests will document the level of friction between the web and the two roller surfaces.

Friction Tests Web/Roller

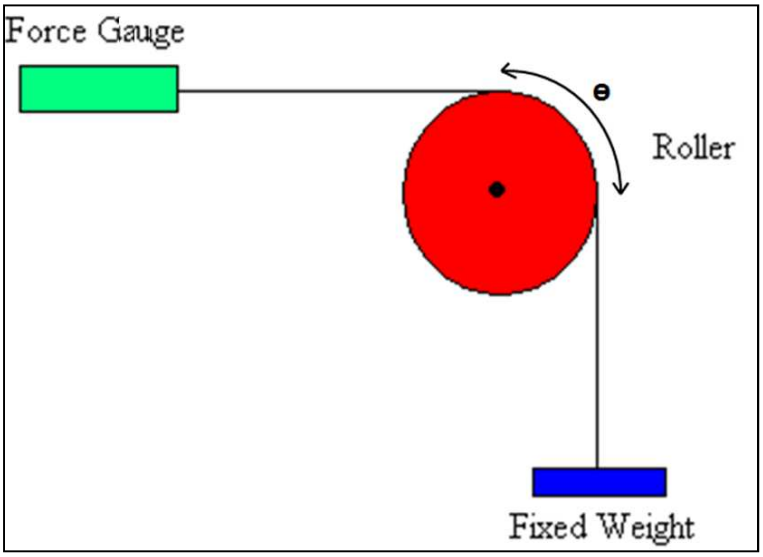

Fig 3.19: Friction test schematic diagram

Using this test, kinetic friction between the web material and the aluminum roller while the web slides over the cylinder (Fig: 3.19) was measured. One end of the web was attached to a known fixed weight and the other end was attached to a force gauge (Mfg: SHIMPO, FCG-5 model). The web was then pulled until it began sliding over a stationary roller surface. Both ends were made to move together so that the web could slide over the cylinder. The fixed weight (T_2) and force gauge (T_1) tensions were recorded and friction coefficient was calculated using the following expressions,

$$\frac{T_1}{T_2} = e^{\mu\theta} \qquad \{2.4\}$$

$$\mu = \frac{ln\frac{T_1}{T_2}}{\theta} \qquad \{2.5\}$$

Where,

T1 – Force gauge reading (Lb)

T2 – Fixed weight (Lb)

μ - Co-efficient of friction.

Θ - Wrap angel of web over the cylinder (Radians).

Co-efficient of friction values of Dow 236 and LDPE web are given in table 3.5,

				Side 1	Side 2					
		Side 1	Side 2	ln(T2/T1)	ln(T2/T1)	θ	μ (Side 1)	Avg μ (Side 1)	μ (Side2)	Avg μ (Side 2)
Temp	T1	T2	T3							
70	1.3	2.72	2.62	0.74	0.7	0.79	0.9		0.9	
	1.3	3.33	3.45	0.94	0.98	0.79	1.2	1.16	1.2	1.15
	1.3	3.75	3.64	1.06	1.03	0.79	1.3		1.3	
100	1.3	2.37	2.47	0.6	0.64	0.79	0.8		0.8	
	1.3	2.66	2.61	0.72	0.7	0.79	0.9	0.81	0.9	0.83
	1.3	2.33	2.41	0.58	0.62	0.79	0.7		0.8	
120	1.3	2.63	2.56	0.7	0.68	0.79	0.9		0.9	
	1.3	2.55	2.28	0.67	0.56	0.79	0.9	0.82	0.7	0.78
	1.3	2.24	2.37	0.54	0.6	0.79	0.7		0.8	

Table 3.5: Co-efficient of friction values of Dow 236 and LDPE

Co-efficient of friction values of bare aluminum roller and LDPE web are given in table 3.6,

				Side 1	Side 2					
		Side 1	Side 2	ln(T2/T1)	ln(T2/T1)	θ	μ (Side 1)	Avg μ (Side 1)	μ (Side2)	Avg μ (Side 2)
Temp	T1	T2	T3							
70	1.3	0.8	0.81	0.49	0.47	1.57	0.31		0.3	
	1.3	0.83	0.79	0.45	0.5	1.57	0.29	0.3	0.32	0.3
	1.3	0.8	0.82	0.49	0.46	1.57	0.31		0.29	
100	1.3	0.88	0.87	0.39	0.4	1.57	0.25		0.26	
	1.3	0.89	0.91	0.38	0.36	1.57	0.24	0.25	0.23	0.24
	1.3	0.87	0.89	0.4	0.38	1.57	0.26		0.24	
120	1.3	0.96	0.91	0.3	0.36	1.57	0.19		0.23	
	1.3	0.93	0.95	0.33	0.31	1.57	0.21	0.21	0.2	0.22
	1.3	0.92	0.91	0.35	0.36	1.57	0.22		0.23	

Table 3.6: Co-efficient of friction values of bare aluminum roller and LDPE

Friction measurements were recorded on both sides of the web on bare aluminum roller and roller with high friction tape. The co-efficient of friction for both cases was appeared to reduce as the temperature increases. Moreover, in both cases, the friction was appeared to be decreased more between 70^{o}F and 100 ^{o}F than it did between 100 ^{o}F and 120 ^{o}F.

Young's Modulus

Young's modulus is the slope of the stress-strain diagram at any point. It will be required as a material input in the finite element modeling discussed in chapter 4. An experiment was conducted by doing stretch test on the LDPE sample. A 10 feet long LDPE sample was cut. One end of the sample was constrained. The other end was held by a force gauge. The sample was then stretched in increments of 0.5 lb until a load of 4 lb was reached. The deformed length was marked at each and every step. The strain and stress were then found from:

$$\epsilon = \frac{\Delta L}{L} \qquad \{2.6\}$$

$$\sigma = \frac{P}{A}\ in^2 \qquad \{2.7\}$$

A = width x thickness. (In our case it is 6 x 0.001 = 0.006 in^2)

Where,

σ - Stress (Psi),

Є – Strain,

P – Load (Lbs) and A – Area (in^2)

E – Young's Modulus (Psi)

The Young's modulus of the web was determined by using a least square fit of a line through the test data. This stretch test was done to find the Young's modulus in the machine direction (E_{MD}). The graph (Fig 3.20) of stress vs. strain for three different trials was plotted. The Young's modulus was determined from the slope of the stress-strain plot.

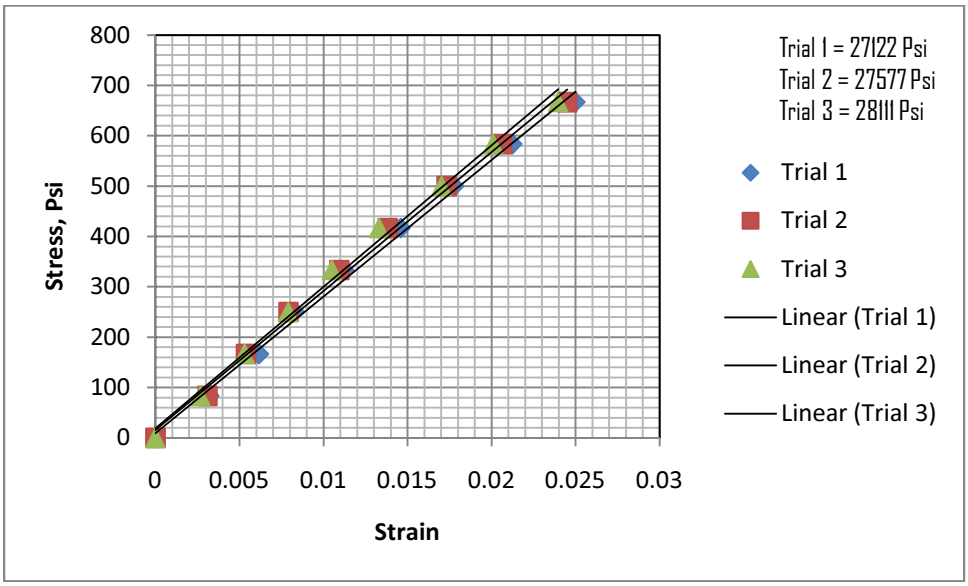

Fig 3.20: Graph for MD Modulus

The Young's modulus in CMD direction was found by cutting the web into 1 inch wide stripes that were 6 inch long in the cross machine direction. Since the sample was very small, the stretch test cannot be done accurately because the resulting deformation was too small to measure by hand. Instron tensile tester shown in Fig 3.21 was used to do this test. The sample was clamped between two clamps on the Instron machine and load was applied gradually in the steps of 0.1 lb until a load of 0.5 lb was attained. A load cell with a capacity of 50 lbs was connected to the strain indicator (3800 wide range strain indicator) from where the strain loads were noted. The change in length was recorded

from a digital display output on the Instron. The graph (Fig 3.22) of stress vs. strain for three different trials was plotted. The Young's modulus can be determined from the slope of the stress-strain plot.

Fig 3.21: Stretch test on Instron machine

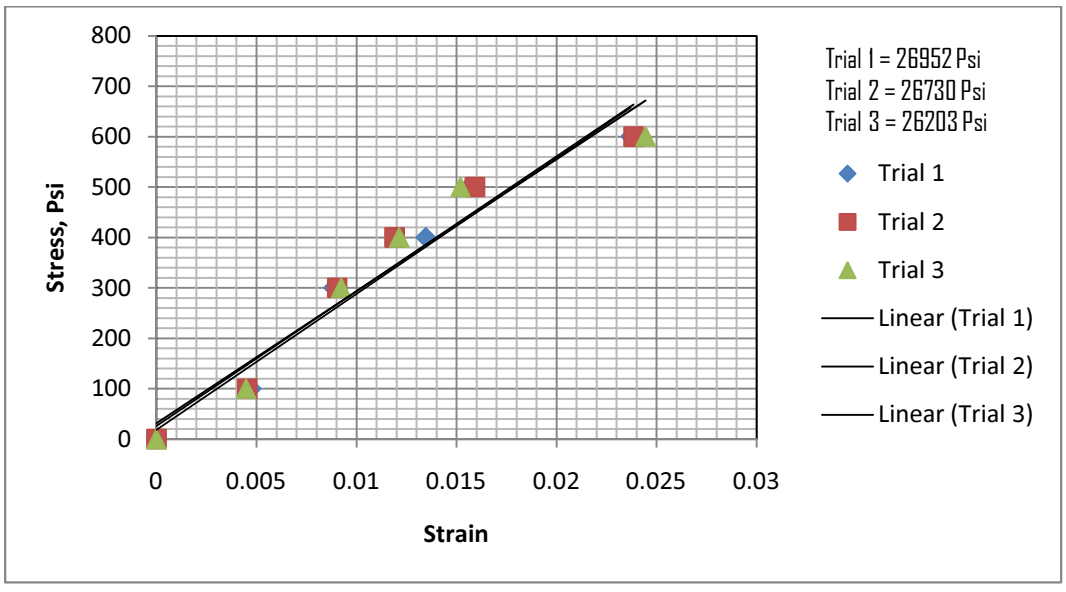

Fig 3.22: Graph for CMD Modulus

From the above Young's modulus tests, it could be concluded that the material was nearly isotropic as it had exhibited almost the same young's modulus in both, MD and CMD. The average value of Young's modulus for this material was determined as 26,500 Psi.

Coefficients of thermal expansion

The thermal expansion coefficients for the LDPE were determined at 3M Company on a TA instrument (model 2840 TMA). This instrument was used to measure thermal expansion coefficients and creep functions on various materials. The samples were heated from 25^{o}C (77^{o}F) to 80^{o}C (176^{o}F) at a rate of 5^{o}C per minute. The results are given in the following table (Table 3.7),

Direction	Ist Heat (x 10^{-6} in/in ^{o}F)	2st Heat (x 10^{-6} in/in ^{o}F)
MD	393	311
CMD	230	52

Table 3.7: Co-efficient of thermal expansions measured in MD and CMD

In the wrinkling tests conducted, the conditions were essentially that of the "1st heat". Tests were conducted on web that was heated once and not reused. The 1st heat expansion coefficient has been used in the analysis

CHAPTER IV

MODELING

The FE model aims to simulate the expansion of web due to heat when passed over a heated roller. The temperature range is 75^{o}F to 120^{o}F. The dashed lines refer to the web nodes passing over the roller, whose lateral deformations have been coupled. These are constrained to enforce normal entry for the web to the roller. All the central nodes of the web center line are constrained in Y direction to prevent rigid body motion. The central node of the left roller is constrained in X direction to avoid singularity error. The Z-displacement, X and Y rotation for all nodes are constrained.

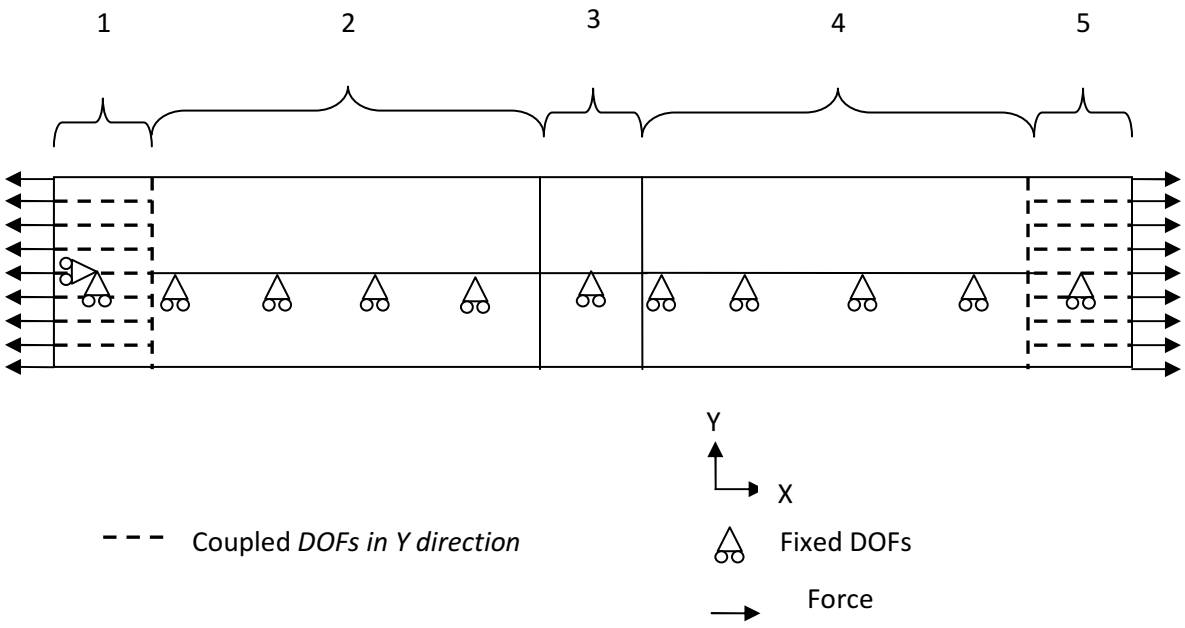

Fig 4.1: Boundary conditions and applied loads.

The above model is divided into five parts. The first part in figure 4.1 is the web on the upstream roller. The second part is the free web span. The third part is the test roller (Hot roller). The fourth and fifth parts are the free web span and the downstream roller respectively.

The FE model employs wrinkling membrane elements for the web in the free spans and the linear elastic elements for the web on the rollers. Wrinkling membrane elements cannot carry compressive stress. The constitutive matrix which relates stress to strain in these elements is dependent on the state of strain in the element. The constitutive matrix can take on one of the three forms including: (1) Taut – for which the principal stresses are both tensile, (2) wrinkled – in which case one principal stress is tensile and second is zero, and (3) slack – in which both in-plane principal stresses are zero. As loads are increased incrementally in a nonlinear solution the principal strains are computed for each element. If $\epsilon_1 > 0$ and $\epsilon_2 > -\vartheta\epsilon_1$, taut conditions are assumed. If $\epsilon_1 > 0$ and $\epsilon_2 < -\vartheta\epsilon_1$, then wrinkled conditions are assumed. If $\epsilon_1 < 0$ slack conditions are assumed to occur. Nodal forces shown at the boundaries of part 1and part 5 are applied to simulate the desired web line tension. Temperature was set at the nodes in the web in contact with the central roller (part 3) which was used to heat the web.

The web is 6” wide LDPE with a thickness of 0.001”. The entry span to hot roller is 30 inches long and exit span is 12 inches long. The diameter of the hot roller was 5.8 inches. The angle of wrap of web over the heated roller is 150 degrees. Young’s modulus is 26,500 psi from the experimental results. The CTE in MD is 0.000393 in/in/^{o}F and 0.00023 in/in/^{o}F in CMD. The web tension applied is 4 lbs which is distributed evenly

across the web width. The model was executed in COSMOSM FEM package developed by Structural Research and Analysis Corporation (SRAC).

All the panels were divided into 20 x 20 elements. There were totally 2814 nodes. Once the model is ready, both static and non-linear analysis was run to predict troughs and wrinkles. For non-linear analysis, two different time curves were used for both tension and temperature loads.

Time curve 1 (Fig 4.2) was associated with the web tension (4 lb).

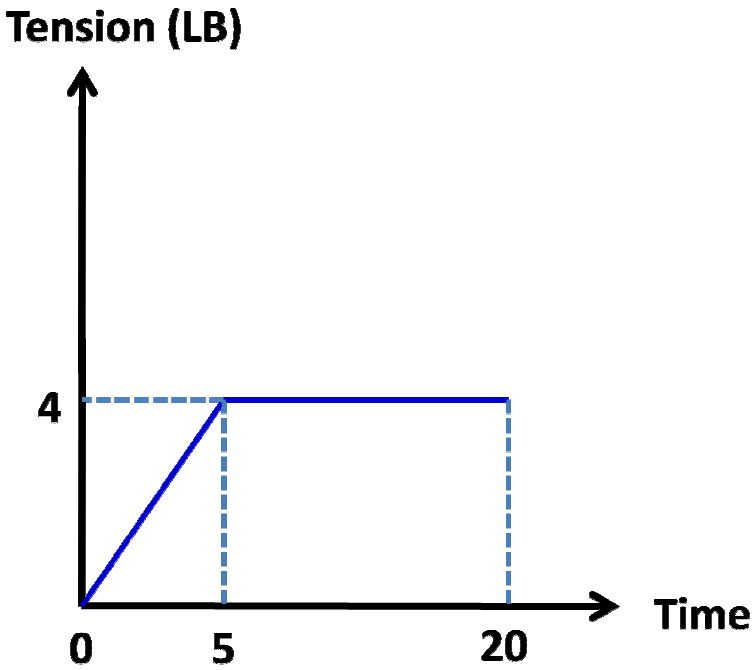

Fig 4.2: Time curve 1 (Tension)

Time curve 2 (Fig 4.3) was associated with temperature loads.

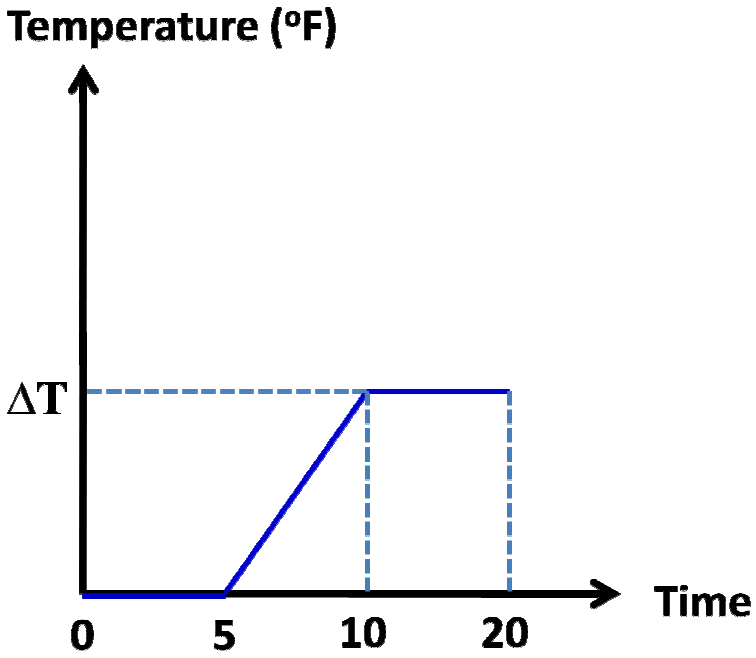

Fig 4.3: Time curve 2 (Temperature)

There were four different cases analyzed.

1) A static analysis case was run setting a ΔT of 5°F to the heated roller. When static analysis are executed, the material behavior of the wrinkle membrane elements is that associated with plane stress in COSMOS. This allows the study of compressive stresses in the free spans (part 2 and 4) where troughs might occur. This simulation was run to check for the formation of troughs on the free span of the web (Part 2) before entering the heated roller (Part 3). The tension applied to both ends of the web is 4 lbs which was evenly distributed evenly across the web width. As expected machine direction stresses of 666.67 Psi result and the web

edge deform inwards 0.02” per side as a result of Poisson contraction. As the stress and displacements matched with the theoretical values, it can be said that the constraints applied to the model are correct.

2) A static analysis was run with applying ΔT of 45 degrees to heated roller and ΔT of 35 degrees for the exit span of web after the heated roller and ΔT of 10 degrees to small portion of web before entering the hot roller as noted in the experiments (Ref : Chapter 3, Dynamic test). In this analysis also it was intended to study the trough formation on the entry span of the web (part 2) at high temperatures. It was evident from the experiments that troughs with higher amplitude formed as temperature increased (ref Fig: 3.13). The FEA stress values and the displacement values were checked with the theoretical values and they were in good agreement.

Again static analyze were done to study trough formation in the free entry span of the web (Part 2) before it entered the hot roller (part 3). The results of this analysis will be discussed in detail in chapter 5. However to study the wrinkling effect, we need to perform non linear analysis or post buckling analysis.

3) Nonlinear analyses with same conditions as case 2 were run with 20 step increment. During the 20 steps the web tension and temperature were increased per Fig 4.2 and 4.3. During each step the principal strains were evaluated and the material behavior of each wrinkle membrane element was reviewed for taut, wrinkled or slack conditions and then was set for the following step. This is similar to the experimental condition where the temperature increases from room temperature to high temperatures like 120 degrees. This simulates the web material passing over the hot aluminum roller. In actual experiment it was

observed that web expands 0.015” in width due to heat from the roller. This will cause the web to have non normal entry to the heated roller. A displacement constraint was enforced at the web edges to simulate this expansion, which is much less than the free CMD expansion for this temperature change (0.00023 * 45 * 6 = 0.062 inches) to check for wrinkles as observed in the wrinkling tests.

4) A nonlinear case with same conditions as case 3, but now the nodes on the heated roller were constrained from expanding in the lateral direction was run with 20 step increments. From the web expansion experiments it was evident that the web expands minimally on the high friction roller (Ref chapter, web expansion test). Again the tension and temperature were independently controlled through the simulation per Figures 4.2 and 4.3. The model simulated LDPE web running over the heated roller with DOW 236 tape on it. This case was run to explore the trough formation, which can be quantified by the width reduction of part 2. The width reduction is affected by the tension, temperature, the lateral displacement constraint of the web on the roller (part 3) and the wrinkle membrane behavior of the elements in the entering span (Part 2). Figure 4.4 shows the dimensions and element groups associated with each part of the model.

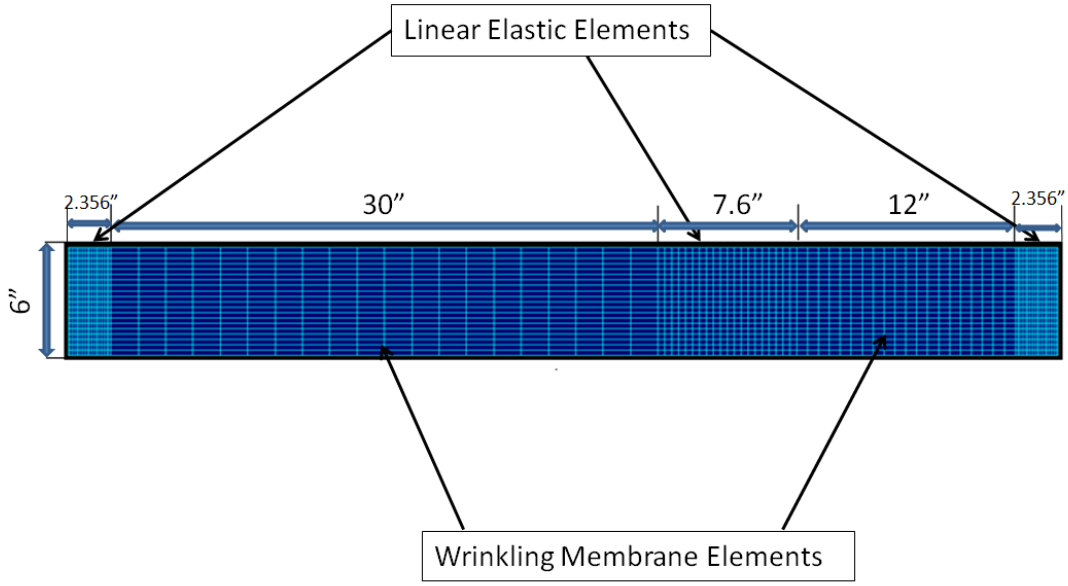

Fig 4.4 – Model dimensions and Element groups.

CHAPTER V

Simulation Results & Discussions

The FE model was executed for wrinkling experiments for a 6" wide, 0.001" thick LDPE web. Young's modulus was determined as 26,500 psi and Poisson's ratio was assumed to be 0.3. The thermal coefficients of expansion are 0.000393 in/in/^{o}F and 0.00023 in/in/^{o}F in MD and CMD directions, respectively. The radius of heated roller is 2.9" and the length of the web spans before and after the heated roller is 30 inches and 12 inches, respectively. A tension of 4 lbs is applied at both ends of the web.

The critical buckling stress for a trough to occur in span entering the heated roller can be calculated by the below formula [4],

$$\sigma_{ycr} = -2\left(\sigma_{e+}\sqrt{\sigma_e^2 + \sigma_e\sigma_x}\right) \qquad \{2.1\}$$

$$\sigma_e = \frac{\pi^2 D}{a^2 h}$$

$$D = \frac{Et^3}{12(1-\vartheta^2)}$$

Input of the test values of the parameters in the above expressions, yields the critical buckling stress to form a trough in the entering web span as: σ_{ycr} = -0.27 psi.

The critical value required to buckle the web on the roller, namely the compressive stress for the onset of wrinkling, can be calculated by Timoshenko shell buckling criteria as shown below [5],

$$\sigma_{ycr} = \frac{-h\,E}{R\sqrt{3(1-\vartheta^2)}} \qquad \{2.3\}$$

Input of the parameters in the above expression yields the critical stress to buckle the web on the roller: σ_{ycr} = -5.53 Psi.

Case 1 results

The first model was a static analysis with a ΔT of just 5^{o}F was applied on the heated roller (Part 3) nodes.

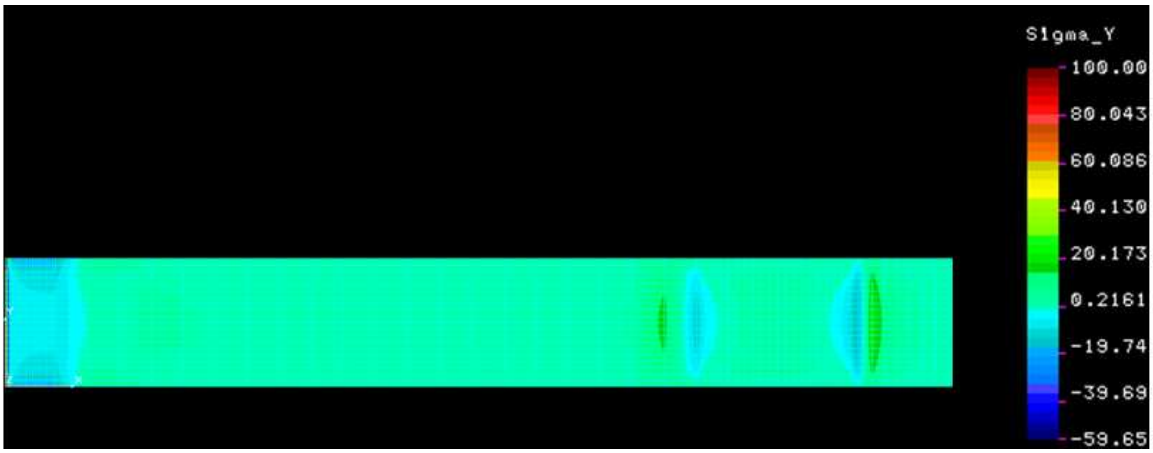

Fig 5.1: Output of CMD stresses on the entry span of the heated roller (ΔT = 5^{o}F).

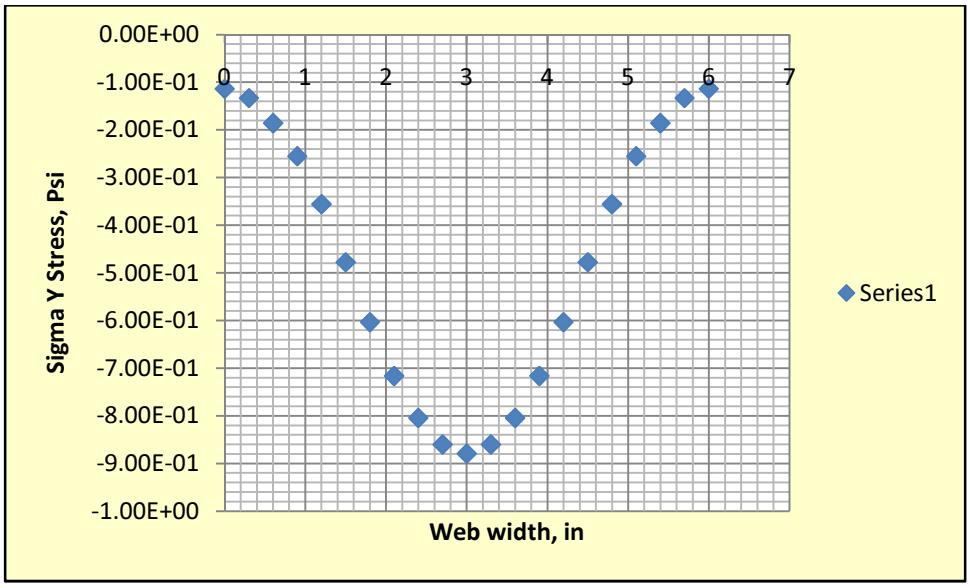

Fig 5.2: Plot of Sy stresses along the web width midway through the entry span (part 2)

In Figure 5.1 the stresses in Y (CMD) direction have been shown in a chart. The stresses in the entry span are small but negative. In an attempt to quantify this variation Figure 5.2 is provided. These stresses are plotted midway through the entry span, 15" from the upstream roller and 15" from the downstream heated roller. As seen in the above Figures 5.1 and 5.2, the CMD stresses occurring at this temperature are in the range of -0.1 to -0.9 Psi which are sufficient to produce troughs over the majority of the web width in entering web span. In experiments the toughs did not become readily visible until the heated roller achieved a temperature of 90^{o}F ($\Delta T = 15^{o}$F), troughs can be very difficult to see in a moving web. Even though the compressive stresses were sufficient to induce troughs, the trough amplitude will be limited by the width reduction of the web in the entry span. To study this width reduction requires the nonlinear analysis which will be reported later.

Case 2 results

A second static case was run where the heated roller temperature was 120^{o}F. The results are shown in Figures 5.3 and 5.4.

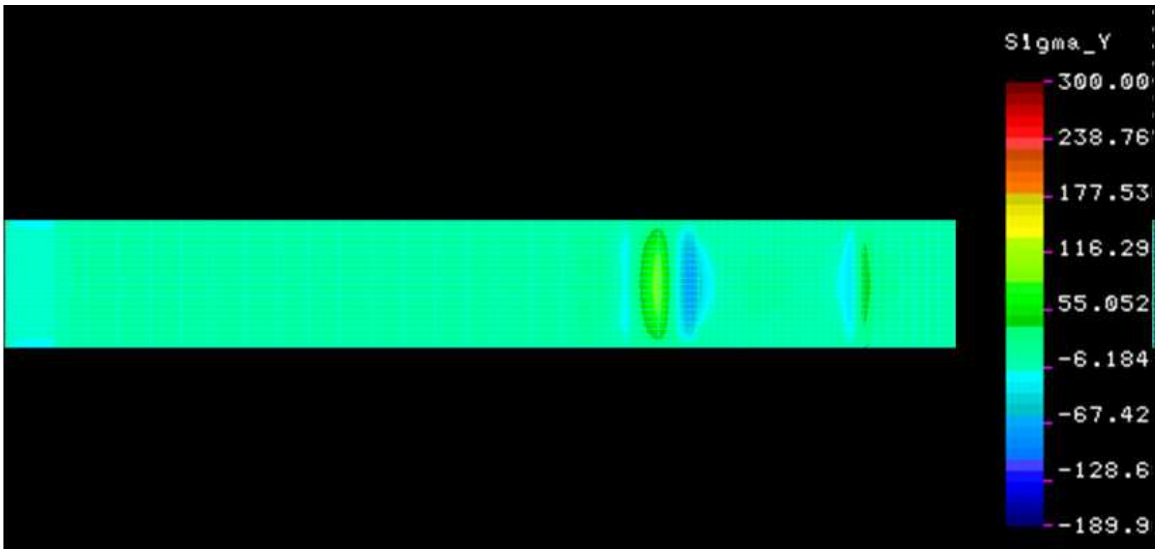

Fig 5.3: Output of CMD stresses on the entry span of the heated roller (ΔT = 45^{o}F).

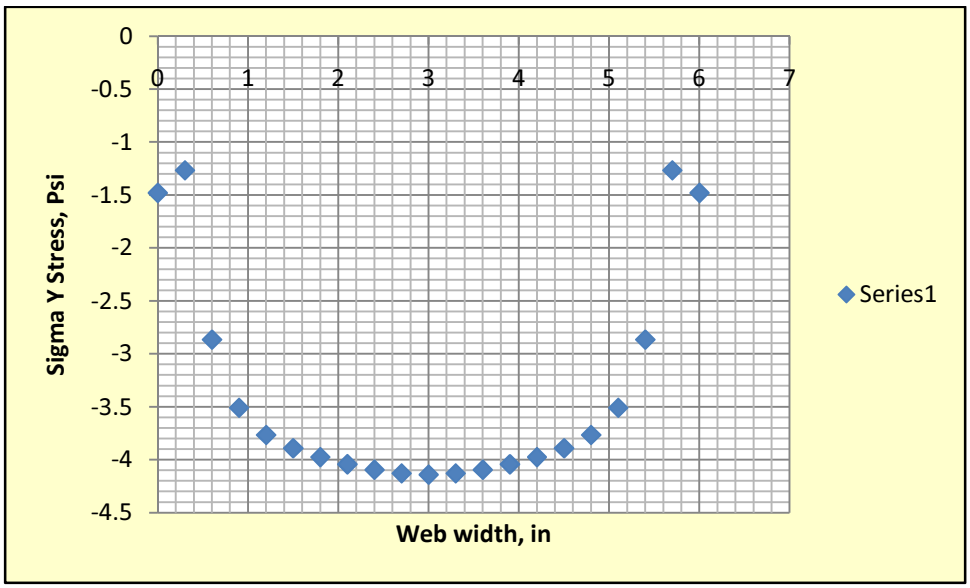

Fig 5.4: Plot of Sy stresses along the web width midway through entry span (Part 2)

From Figures 5.3 and 5.4 we can see the range of CMD stress is from -1.5 to -4.14 psi which is more than sufficient to generate troughs in the entry span (Part 2).

Case 3 results

A nonlinear analysis was run with 20 time intervals, with the tension coming up fully in the 5th interval and temperature coming up fully at 10th step. This analysis allowed the wrinkling membrane behavior in the entry (Part 2) and the exit (part 4) spans. The edge nodes of the heated roller (Part 3) were given a displacement constraint of ±0.0175". This displacement constraint was enforced to allow the combination of the Poisson contraction of the web which is 0.045" and the expansion of 0.01" witnessed in actual tests (Ref: Chapter 3, Web expansion test). Also the temperatures measured at the exit span of the heated roller (Part 4) and entry span (part 2) were also incorporated in the model as measured in tests (Ref :Chapter 3, dynamic test).

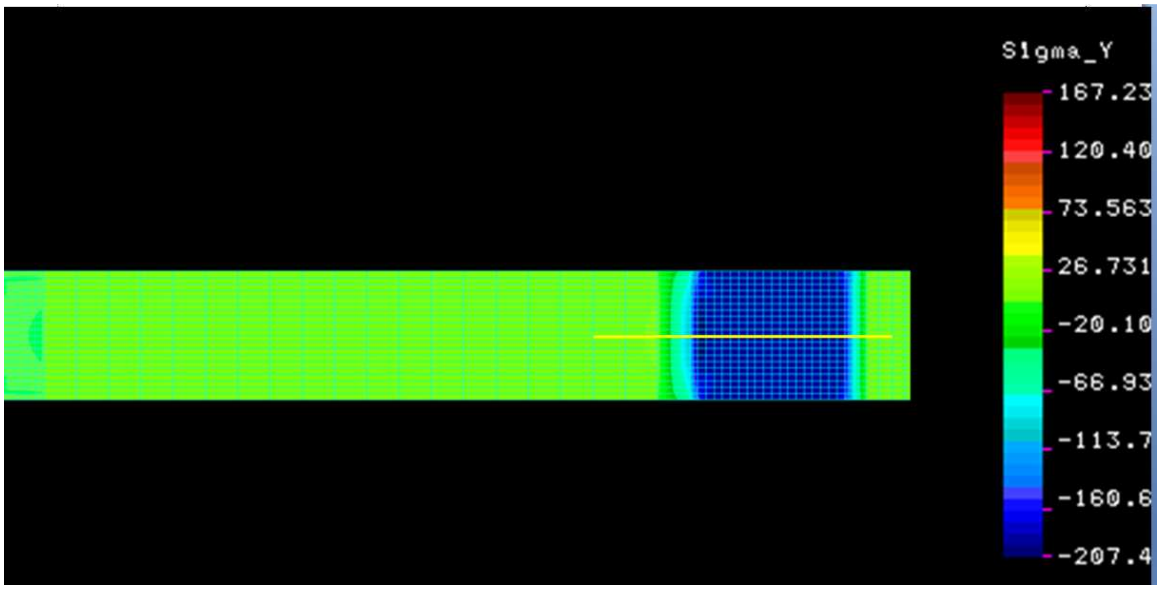

Fig 5.5: Output of CMD stresses on the entry span of the heated roller and on the heated roller ($\Delta T = 45^{o}F$) - non linear.

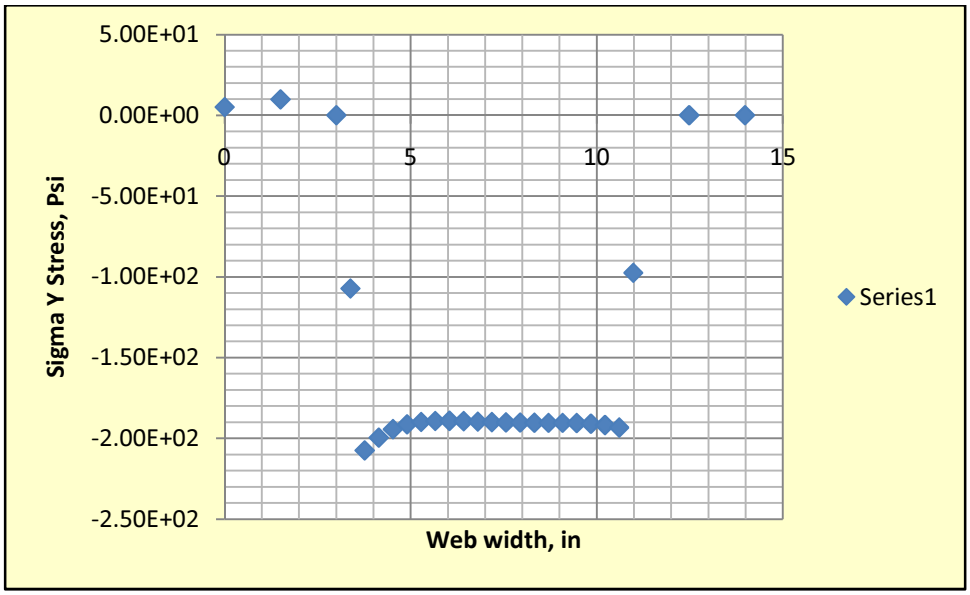

Fig 5.6: Plot of Sy stresses on the heated roller (Part 3, Along the yellow line of fig 5.5)

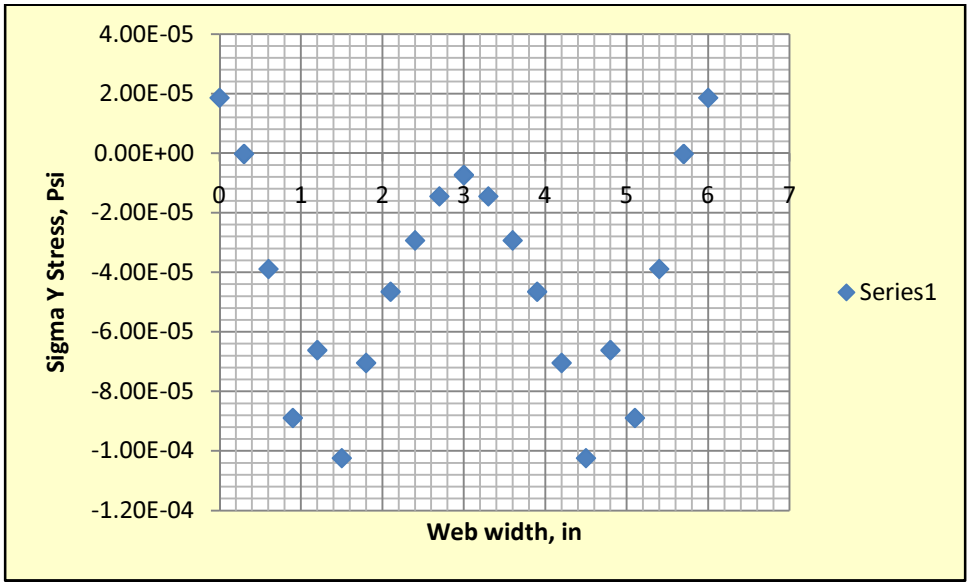

Fig 5.7: Plot of Sy stresses along the web width midway through entry span (Part 2)

Here (fig 5.7) the CMD stresses before the entry of the heated roller is very small. However there are high CMD stresses just before the entry to heated roller. We can also notice very high compressive stresses at the entry to and on the roller which are more than sufficient to form a buckle or wrinkle (fig 5.5 & 5.6). The web actually expands

when heated. Since wrinkling membrane elements cannot carry compression, we witness no compressive stress in the web entry span. Also the web does not enter normally over the heated roller due to thermal expansion. The tension in machine direction and the expansion in cross machine direction generate high stresses at the entry of the roller. But in real case as the web expands and creates a non normal entry, the outer edges of the web steer inward to generate troughs and wrinkles. This was captured in chapter 3 in the wrinkling experiments. The high degree of CMD compressive stresses on the roller indicates that wrinkles should occur as temperature is increased. However, as we shall see, negative CMD stresses more negative than the critical Timoshenko buckling stress are not sufficient grounds to claim that wrinkling has occurred.

Theoretically, the free expansion of the web in the CMD for the above model due to increased temperature would have been,

$$\Delta W = \Delta T * \alpha * w$$

= 45 * 0.00023 * 6 = 0.062 “.

In tests the web expanded only 0.01”. It is obvious friction is constraining this expansion. Also the Poisson contraction for this web without any temperature loads can be calculated by,

$$\Delta W = -\vartheta * \epsilon_{CMD} * w$$

= -0.3 * 0.02515 * 6 = -0.045

Where,

ΔW – Change in web width

ΔT – Change in temperature.

α – Coefficient of thermal expansion

w – Web width

ε_{CMD} – Lateral strain

υ – Poisson ratio

The same model was analyzed by having ΔT as zero and removing the constraints on the heated roller (Part 3) edge nodes. Here the web width reduction (w_1) is due to only Poisson contraction. Below shown is the plot (Fig 5.7) of the Y-displacements of this model at the center of the entry span (Part 2).

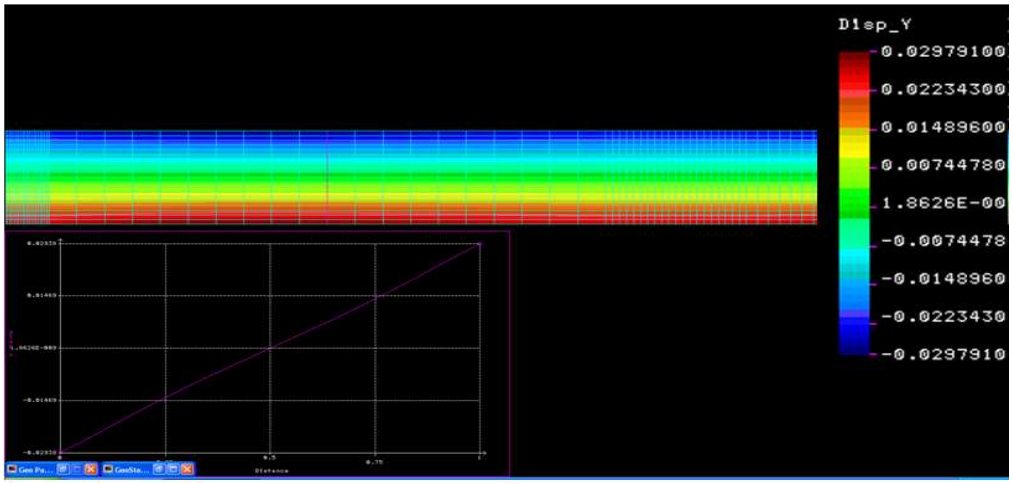

Fig 5.8: Y-Displacements at center of the entry span (part 2), ($\Delta T = 0^oF$).

Form these Y-displacements, it was calculated that web was contracted to a width of 5.94124" (w_1). This reduction in width is due to Poisson contraction. The Y-displacements in the previous model was also measured in the same location and the width reduction of 5.9169" (w_2) was found. Below shown is the plot (Fig 5.8) of Y-displacements with $\Delta T = 45^oF$.

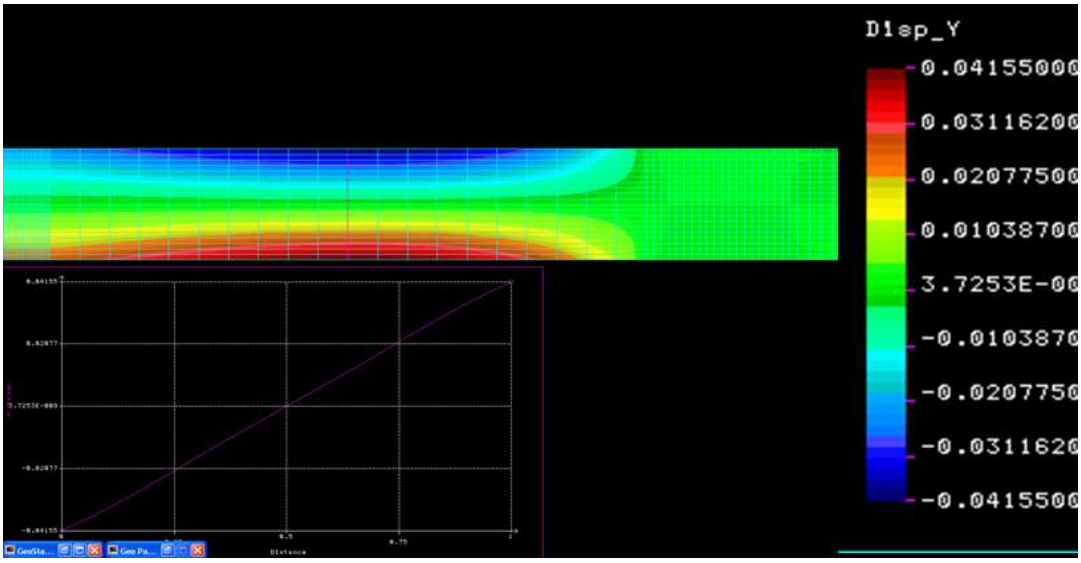

Fig 5.9: Y-Displacements at center of the entry span (part 2), ($\Delta T = 45^{o}F$).

The difference in these two widths (w_1 - w_2) is 0.0243". The difference in web width is a measure of the degree to which the web is not in normal entry to the heated roller. The closer this number is to zero, the closer the web will be to the normal entry boundary condition. The web will attempt to dynamically steer into normal entry such that this change in width will be eliminated. The fact that each edge will steer inward 0.012 inches combined with the high negative CMD stresses witnessed in Fig 5.5 and 5.6 produce the wrinkles witnessed in testing. To witness instability requires:

1) Stresses to be created that are more negative than that predicted by Timoshenko's algorithm (Equation 2.3)
2) A mechanism by which the width of the web compresses, in this case the non-normal entry caused by the heated roller. This in-plane deformation becomes out-of-plane deformation in the form of a wrinkle.

Case 4 results

Further proof that this hypothesis was correct was provided by case 4. This final model was to simulate the roller with high friction tape (Dow 236) where the web was entering normally on the heated roller and was not able to expand due to high friction between web and the roller surface. To simulate this condition, all the edge nodes of the web on the heated roller surface were constrained to Poisson contraction value (±0.0225") since no expansion was witnessed in tests (Chapter3, wrinkling experiments). Also the temperatures measured at the exit span of the hot roller (Part 4) and entry span (part 2) were also incorporated in the model as measured in tests (Chapter 3, dynamic test).

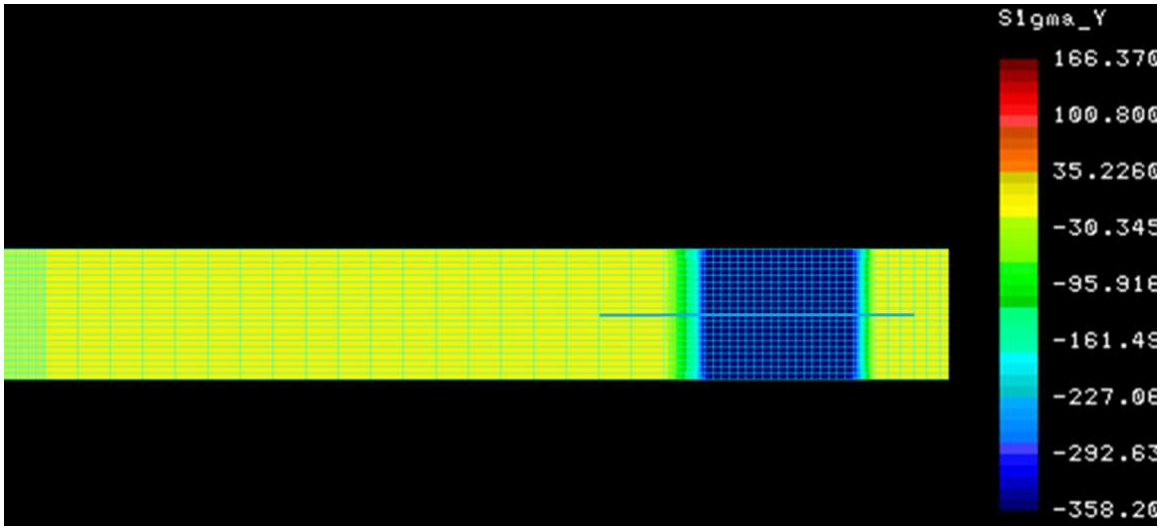

Fig 5.10: Output of CMD stresses on the entry span of the heated roller and on the heated roller ($\Delta T = 45^{o}F$) - non linear (Normal entry).

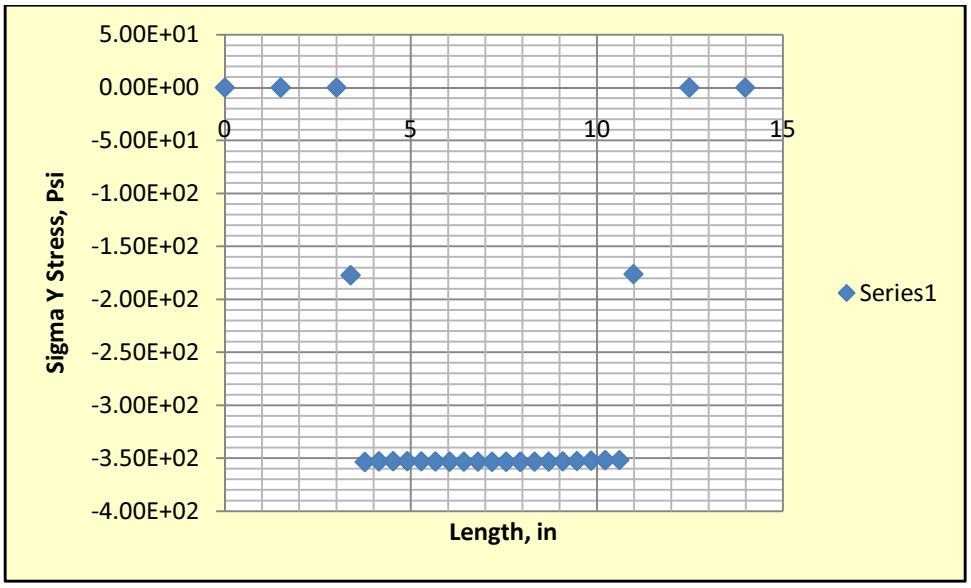

5.11: Plot of Sy stresses on the heated roller (Part 3, along the blue line of Fig 5.10)

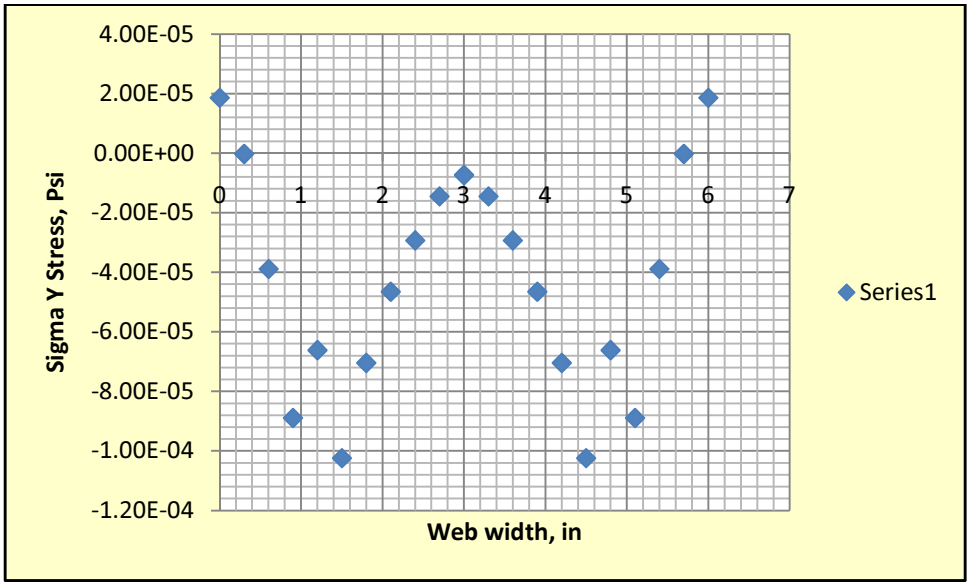

Fig 5.12: Plot of Sy stresses along the web width midway through the entry span (part 2)

The CMD stresses (5.12) are again small across the whole span before entering the roller. This again is the result of the wrinkle membrane elements incapacity to withstand compressive stress. There are very high compressive stresses of the order -350 psi on the roller surface. As shown in fig 5.11 these negative stresses are even more

negative than those witnessed for bare heated roller (fig 5.6). Thus it would seem that the high friction case should produce even more wrinkling, but this was shown not to be the case in testing (Chapter 3, wrinkling experiments).

Again the explanation for this behavior is provided by exploring the lateral deformations induced in the web by the heated roller. The Y-displacements (Fig 5.13) were checked at the middle of the entry span (part 2). The reduced web width was 5.93146" (w_3). Below shown is the figure of the Y-displacements at mid-span,

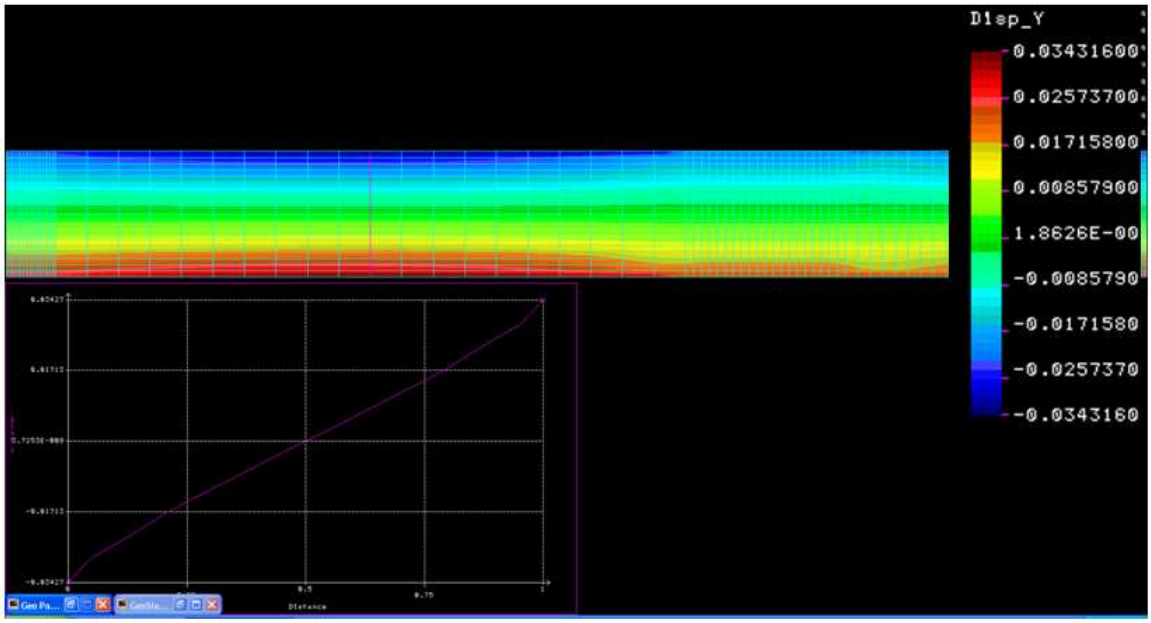

Fig 5.13: Y-Displacements at center of the entry span (part 2), ($\Delta T = 45^{o}F$), High friction Case.

The difference between the web width due to Poisson contraction and the above model (w_1 - w_3) is 0.00978", about 2.4 times smaller than the change in width for the bare low friction case. Thus the web approaching the heated roller for the high friction case 4 is much closer to normal entry conditions than the web in case 3 where the friction was much lower. With less lateral deformation of the web there was less out-of-plane deformation and no wrinkles were visible in tests.

CHAPTER VI

Conclusions

Experiments were conducted on LDPE web to study the formation of troughs and wrinkles due to heat while passing over the heated rollers. The same boundary conditions as in actual experimental setup were used in the FE model and both static and non-linear analyses were performed. Following are the conclusions drawn from this research,

1) The LDPE webs attain the roller temperature instantaneously due to their low thermal mass. This is true for both bare aluminum roller and roller with high friction tape (Dow 236). The data from Tables 3.1, 3.2, 3.3 & 3.4 show the thermal conductivity between web and the bare aluminum roller/roller with high friction tape was good.

2) These webs expand while passing over the heated rollers. This was captured in the web expansion experiments in Chapter 3. However friction opposes the web expansion. On bare aluminum heated roller, the web should expand by 0.062" due to a ΔT of $45^{o}F$. In actual tests, the web expanded only 0.01". Also when the web was passed over the heated roller with high friction tape, no lateral expansion was observed. This observation shows friction restrains the web lateral expansion on the heated rollers. The data from Tables 3.5 and 3.6, show the coefficient of friction values between web/roller with high friction tape ($\mu = 1.1$) and web/bare aluminum roller ($\mu = 0.3$). As the temperature increased, there was a drop in coefficient of friction. In bare aluminum roller case it went down to $\mu=0.2$. Hence

troughs of higher amplitudes formed at the entry span of web due to web expansion. However in high friction roller case, friction coefficient went down to μ=0.8, which is still very high. Hence no web expansion was observed, in turn no troughs and wrinkles were observed.

3) Wrinkling experiments show that troughs form at the entry span before the heated roller. As temperature increased to 120^{o}F, large number of troughs with higher amplitude was noticed at the entry span. Tiny wrinkles formed on the surface of the heated roller. This is because the web enters the heated roller in a non normal entry which results in steering the outer edges of web inward leading to formation of troughs at entry span and wrinkles on the roller surface. However on high friction tape roller, even at higher temperatures, no troughs or wrinkles formed. Here friction prevents expansion of web and hence web enters normally on to the heated roller. This provides no inbound steering on the web edges and hence no troughs or wrinkles are formed.

4) The critical buckling stress to form troughs in the free span of this FE model is calculated to be, σ_{ycr} = -0.27 Psi. The static analysis result show that, for both ΔT=5^{o}F (fig 5.1 & 5.2) and ΔT=45^{o}F (fig 5.3 & 5.4), there is sufficient compressive stresses in the free entry span (part 2) to generated troughs.

5) The critical buckling stress to form a wrinkle on the heated roller of the FE model is calculated to be, σ_{ycr} = -5.53 Psi. The non linear analysis which simulates bare aluminum roller condition (Model 3) shows high compressive stresses on the roller surface (Fig 5.5) which are more than sufficient to generate wrinkles on the roller. However to find the trough formation at the free span before the heated

roller, the width reduction at the center of the free span is checked (w_2). The width reduction (w_1) at center of the free span due to Poisson contraction at $\Delta T = 0^oF$ was also checked. The difference between those width reductions (w_1-w_2) was 0.02434". This value is the amount of out-of-plane deformation of the web which is in the form of trough that will induce wrinkle on the heated roller.

6) The non-linear analysis which simulates the roller with high friction tape -Dow 236 (model 4) where the web enters normally on the heated roller also shows very high compressive stresses (Fig 5.9) on the heated roller which are more than sufficient to induce wrinkles. The width reduction (w_3) in this case was also calculated at the center of the entry span. The difference between width reductions (w_1-w_3) was found to be 0.00978". This is very tiny value and troughs forming due to this out-of-plane deformation get flattened on the roller surface. As seen in experiment, no troughs form at the entry span of the web. Although there are very high compressive stresses on the roller surface, there are no troughs in entry span of the web which could form wrinkles on the roller.

7) This research has proven that there are two requirements that must be satisfied to produce web wrinkles due to elevated roller temperatures. First, the change in web temperature combined with friction must be sufficient to produce CMD stresses that are more negative than the Timoshenko buckling stress (2.3). Second, the temperature change must be sufficient to produce a reduction in web width in the entry span that will promote out-of-plane deformation (wrinkles) in the web on the roller.

Future Work

In this research, the effect of temperature on LDPE webs passing over heated rollers was studied. Further, both thermal and instability analysis can be conducted with an ABAQUS Explicit code. This will prevent us from applying the enforced displacement boundary conditions. The effect of web/roller friction limiting the expansion of the web would occur naturally in such a model. Also the web would seek normal entry.

REFERENCES

1) Sheldon.J.J, “Lateral dynamics of a moving Web”, PhD.Thesis, OSU, 1968
2) Friedrich, C.R and Good, J.K., “Stability sensitivity of a web wrinkles on rollers”, TAPPI Journal, PP 161-165, Feb, 1989.
3) Genlbach, L.S; Good, J.K, and Kedl, D.M, “Prediction of shear wrinkles in Web Span”, TAPPI Journal, Vol 72, No.8, P: 129-134, Aug 1989.
4) Good, J.k and Biesel, J.A, “Instability of Web: The prediction of troughs and wrinkles” advances in pulp and paper research oxford 2009 vol. pp 517.
5) S.Timoshenko, S.P, Gere,J.M, Theory of elastic stability, 2nd edition McGraw-Hill, 1961, P: 324-332.
6) Sheldon, J.J, “Buckling of webs from lateral compressive forces”, proceedings of second International web conference, Stillwater, WHRC, OSU, June 1993.
7) Bensen, R.C ;et al, “Simulation of wrinkling patterns in webs due to non-uniform transport conditions”, proceedings of second international conference on web handling, Stillwater, Ok, WHRC, OSU, June 1993.
8) Good, J.K and Stranghar,P, “Wrinkling of webs due to twist”, proceedings of the 5th international conference on web handling, Stillwater, Ok, WHRC, OSU, June 1999.
9) Webb,D.K, “Prediction model of proper-web working and some numerical calculation examples with experimental verifications”, Proceeding of the eight international conference on web handling, Stillwater, Ok, WHRC, OSU, 2005
10) Beisel, J.A , “ Single span web buckling due to roller imperfections in the web process machining”, PhD thesis, OSU, Dec – 2006

11) Mallya, Sandesh, “Investigation of the effects of voids on the stability of webs”, M.S.Thesis, OSU, July 2008

12) Kara, Ishan, “Wrinkling formation due to non-uniform length across the width of a web”, M.S.thesis, OSU, July 2008.

Appendix – A

Finite Element Models

COSMOS 2.8 is the FE package used to model this problem. First a new file is created to start this modeling. A blank screen with the coordinate axis appears. Proper plane is selected to give the co-ordinates for the model. The major length and width Co-ordinates are specified using points. These points are then connected using curves. Surface command is used to create one surface from these connected curves. Then the element groups are specified. For all the parts of the model, SHELL4 element was used. However, the roller elements were specified as linear elastic elements and the web spans were specified as wrinkling membrane elements. Apart from that all other default setting were used. Then material properties like E, υ, α_{MD} and α_{CMD} were entered. The thickness was given as 0.001" in the real constants. A parametric mesh was done across the whole model dividing all the panels into 40 x 40 elements. The nodes were then merged using the NMERGE command within a tolerance of 0.0001. In total there were 2184 nodes in the model. The nodes of the upstream and downstream rollers were coupled in lateral direction to ensure normal entry of the web. All nodes were constrained in Z displacement, X & Y rotations. All the central nodes of the web in MD direction were constrained in Y-direction to prevent rigid body motion. A load of 4lb was applied on both sides of the web equally distributing the load on all nodes. The loads were associated with time curve 1 and temperature loads applied were associated to time curve 2. The reference temperature was specified as 75°F. The time curves were divided into 20 steps with an increment of 1. The tension will come up at the 5^{th} step. The temperature loads will fully be applied in the 10^{th} step. All other COSMOS settings were kept

unchanged. The force control technique used was Newton Raphson method instead of the default Modified Newton Raphson method.

Below shown is a session file of case 4,

VIEW,0,0,1,0

PT,1,0,0,0

PT,2,2.356,0,0

PT,3,32.356,0,0

PT,4,39.956,0,0

PT,5,51.956,0,0

PT,6,54.312,0,0

PT,7,0,6,0

PT,8,2.356,6,0

PT,9,32.356,6,0

PT,10,39.956,6,0

PT,11,51.956,6,0

PT,12,54.312,6,0

CRLINE,1,1,7

CRLINE,2,2,8

CRLINE,3,3,9

CRLINE,4,4,10

CRLINE,5,5,11

CRLINE,6,6,12

SF2CR,1,1,2,0

SF2CR,2,2,3,0

SF2CR,3,3,4,0

SF2CR,4,4,5,0

SF2CR,5,5,6,0

EGROUP,1,SHELL4,2,0,0,0,0,0,0,0

RCONST,1,1,1,7,0.001,0,0,0,0,0,1E-008

MPROP,1,EX,21600.

MPROP,1,EY,21600.

MPROP,1,NUXY,0.3

MPROP,1,ALPY,0.00023

MPROP,1,ALPX,0.000393

M_SF,1,5,2,4,20,20,1,1

EGROUP,2,SHELL4,2,1,0,0,10,0,0,0

MPROP,2,ALPY,0.00023

MPROP,2,ALPX,0.000393

MPROP,2,EX,21600.

MPROP,2,EY,21600.

MPROP,2,NUXY,0.3

M_SF,2,4,2,4,20,20,1,1

NMERGE,1,2205,1,0.0001,0,1,0

CPDOFND,1,UY,1,1,421,21

C* Total of 3 CPDOF sets defined starting from 1.

CPDOFND,4,UY,2,2,422,21

C* Total of 3 CPDOF sets defined starting from 4.

CPDOFND,7,UY,3,3,423,21

C* Total of 3 CPDOF sets defined starting from 7.

CPDOFND,10,UY,4,4,424,21

C* Total of 3 CPDOF sets defined starting from 10.

CPDOFND,13,UY,5,5,425,21

C* Total of 3 CPDOF sets defined starting from 13.

CPDOFND,16,UY,6,6,426,21

C* Total of 3 CPDOF sets defined starting from 16.

CPDOFND,19,UY,7,7,427,21

C* Total of 3 CPDOF sets defined starting from 19.

CPDOFND,22,UY,8,8,428,21

C* Total of 3 CPDOF sets defined starting from 22.

CPDOFND,25,UY,9,9,429,21

C* Total of 3 CPDOF sets defined starting from 25.

CPDOFND,28,UY,10,10,430,21

C* Total of 3 CPDOF sets defined starting from 28.

CPDOFND,31,UY,11,11,431,21

C* Total of 3 CPDOF sets defined starting from 31.

CPDOFND,34,UY,12,12,432,21

C* Total of 3 CPDOF sets defined starting from 34.

CPDOFND,37,UY,13,13,433,21

C* Total of 3 CPDOF sets defined starting from 37.

CPDOFND,40,UY,14,14,434,21

C* Total of 3 CPDOF sets defined starting from 40.

CPDOFND,43,UY,15,15,435,21

C* Total of 3 CPDOF sets defined starting from 43.

CPDOFND,46,UY,16,16,436,21

C* Total of 3 CPDOF sets defined starting from 46.

CPDOFND,49,UY,17,17,437,21

C* Total of 3 CPDOF sets defined starting from 49.

CPDOFND,52,UY,18,18,438,21

C* Total of 3 CPDOF sets defined starting from 52.

CPDOFND,55,UY,19,19,439,21

C* Total of 3 CPDOF sets defined starting from 55.

CPDOFND,58,UY,20,20,440,21

C* Total of 3 CPDOF sets defined starting from 58.

CPDOFND,61,UY,21,21,441,21

C* Total of 3 CPDOF sets defined starting from 61.

CPDOFND,64,UY,883,883,1303,21

C* Total of 3 CPDOF sets defined starting from 64.

CPDOFND,67,UY,884,884,1304,21

C* Total of 3 CPDOF sets defined starting from 67.

CPDOFND,70,UY,885,885,1305,21

C* Total of 3 CPDOF sets defined starting from 70.

CPDOFND,73,UY,886,886,1306,21

C* Total of 3 CPDOF sets defined starting from 73.

CPDOFND,76,UY,887,887,1307,21

C* Total of 3 CPDOF sets defined starting from 76.

CPDOFND,79,UY,888,888,1308,21

C* Total of 3 CPDOF sets defined starting from 79.

CPDOFND,82,UY,889,889,1309,21

C* Total of 3 CPDOF sets defined starting from 82.

CPDOFND,85,UY,890,890,1310,21

C* Total of 3 CPDOF sets defined starting from 85.

CPDOFND,88,UY,891,891,1311,21

C* Total of 3 CPDOF sets defined starting from 88.

CPDOFND,91,UY,892,892,1312,21

C* Total of 3 CPDOF sets defined starting from 91.

CPDOFND,94,UY,893,893,1313,21

C* Total of 3 CPDOF sets defined starting from 94.

CPDOFND,97,UY,894,894,1314,21

C* Total of 3 CPDOF sets defined starting from 97.

CPDOFND,100,UY,895,895,1315,21

C* Total of 3 CPDOF sets defined starting from 100.

CPDOFND,103,UY,896,896,1316,21

C* Total of 3 CPDOF sets defined starting from 103.

CPDOFND,106,UY,897,897,1317,21

C* Total of 3 CPDOF sets defined starting from 106.

CPDOFND,109,UY,898,898,1318,21

C* Total of 3 CPDOF sets defined starting from 109.

CPDOFND,112,UY,899,899,1319,21

C* Total of 3 CPDOF sets defined starting from 112.

CPDOFND,115,UY,900,900,1320,21

C* Total of 3 CPDOF sets defined starting from 115.

CPDOFND,118,UY,901,901,1321,21

C* Total of 3 CPDOF sets defined starting from 118.

CPDOFND,121,UY,902,902,1322,21

C* Total of 3 CPDOF sets defined starting from 121.

CPDOFND,124,UY,903,903,1323,21

C* Total of 3 CPDOF sets defined starting from 124.

DND,1,UZ,0,2184,1,RX,RY,

DND,11,UY,0,431,21,

DND,1355,UY,0,1733,21,

DND,1796,UY,0,2174,21,

DND,452,UY,0,872,21,

DND,893,UY,0,1313,21,

DND,221,UX,0,221,1,

CURDEF,TIME,1,1,0,0,5,1,20,1

FND,2,FX,-0.19047619,20,1

FND,1,FX,-0.095238095,1,1

FND,21,FX,-0.095238095,21,1

FND,1303,FX,0.095238095,1303,1

FND,1323,FX,0.095238095,1323,1

FND,1304,FX,0.19047619,1322,1

DND,462,UY,-0.0225,882,21,

DND,442,UY,0.0225,862,21,

CURDEF,TIME,2,1,0,0,5,0,10,1,20,1

TREF,75

NTND,442,120,882,1

NTND,1786,110,2184,1

NTND,1702,85,1743,1

TIMES,0,20,1

STRAIN_OUT,1,1,1,0,1,1

NL_CONTROL,0,1

NL_PLOT,1,20,1,0

A_NONLINEAR,S,1,1,20,0.01,0,T,0,0,1E+010,0.01,0.01,0,1,0,0

C* R_NONLINEAR

VITA

Saikiran Divakaruni

Candidate for the Degree of

Master of Science

Thesis: WRINKLING OF WEBS APPROACHING HEATED ROLLERS

Major Field: Mechanical & Aerospace Engineering

Biographical:

Personal Data : Born in Vijayawada, Andhra pradesh, India, on May 10, 1985, the son of Satyanarayana Divakaruni and Sesha lakshmi Divakaruni.

Education:

Completed the requirements for the Master of Science in Mechanical and Aerospace Engineering at Oklahoma State University, Stillwater, Oklahoma in May, 2011.

Received Bachelor of Engineering in Mechanical Engineering, from Anna university, Chennai, India, in May 2006.

Experience:

Graduate Research Assistant in Mechanical & Aerospace Engineering at Oklahoma state university, Stillwater, Feb 2009 to Present.

Graduate Teaching Assistant in Mechanical & Aerospace Engineering at Oklahoma state university, Stillwater, Aug 2010 to Present.

Product Design Engineer in R& D at Brakes India Ltd, Chennai, India, Jun 2006 to July 2008

Name: SAIKIRAN DIVAKARUNI Date of Degree: May, 2011

Institution: Oklahoma State University Location: Stillwater, Oklahoma

Title of Study: WRINKLING OF WEBS APPROACHING HEATED ROLLERS

Pages in Study: 67 Candidate for the Master of Science

Major Field: Mechanical & Aerospace Engineering

Scope and Method of Study: There are several reasons webs wrinkle when passing over rollers. Some of the reasons for wrinkles on web are roller misalignment, tapered rollers, decrease in web tension, difference in web thickness etc. The scope this research is to investigate web instability due to the effect of temperature on web material passing over a heated roller. A heated roller was setup on the small scale web transport machine. Wrinkling experiments were run by passing LDPE web material over the heated aluminum roller in bare condition and also with high friction tape. Input parameters like Young's Modulus, web lateral expansion value required for FE simulations was also found by tests. Both static and non-linear FE simulations were performed and results were compared with the experimental observations and theoretical calculations.

Findings and Conclusions: Experimental results show the LDPE web expands on a bare aluminum roller. Troughs are generated on entry span of the heated roller. Wrinkles are formed on the heated roller surface. In high friction case, no troughs or wrinkles are observed. The static and non-linear FE simulation results correlated well with the experimental observations and theoretical calculations. It has been shown herein that, web instabilities like troughs and wrinkles can be generated on these LDPE webs due to increase in temperature. On bare aluminum roller, the web has a non normal entry due to expansion which results in steering of outer edges inward leading to formation of troughs on the entry span and then finally wrinkles on roller surface. In high friction roller case, the outer edges on the heated roller do not expand due to high friction, which provide no inward steering and hence no troughs or wrinkles are formed.

ADVISER'S APPROVAL: Dr.James.K.Good